Chapter 2
Accretion Disc Winds

A view of space, with an elephant obstructing it

Mike Vennart, Silent/Transparent

2.1 Observational Evidence

Observational evidence for mass-loaded outflows or winds is widespread across the entire astrophysical mass range and most of the electromagnetic spectrum. Before exploring this evidence, it is pertinent to briefly discuss the 'smoking gun' used to unambiguously detect winds—the presence of blue-shifted BALs or 'P-Cygni' profiles in an object's spectrum.

Figure 2.1 shows how a spherical outflow presenting significant line opacity will cause these characteristic profile shapes to form, as scattering out of the line of sight causes a dip in the blue wing of the line, while scattering into the line of sight from other portions of the outflow causes an increase in flux in the red wing of the line. The situation is much more complex in most astrophysical situations; for example, the geometry is rarely spherically symmetric, and the line is rarely a pure scattering case. Indeed, the potential for complicated radiative transfer effects and the variety in line formation mechanisms (e.g. recombination, collisional excitation) is one of the reasons why 3D Monte Carlo radiative transfer simulations are necessary to effectively model disc winds (see Chap. 3).

2.1.1 Cataclysmic Variables

It has been known for a long time that winds emanating from accretion discs are important in shaping the ultraviolet (UV) spectra of high-state CVs (Heap et al. 1978; Greenstein and Oke 1982). The most spectacular evidence for such outflows are the P-Cygni-like profiles seen in UV resonance lines such as C IV 1550 Å (e.g. Cordova and Mason 1982, see Fig. 2.2). Considerable effort has been spent over the

J. Matthews, *Disc Winds Matter*, Springer Theses,
DOI 10.1007/978-3-319-59183-4_2

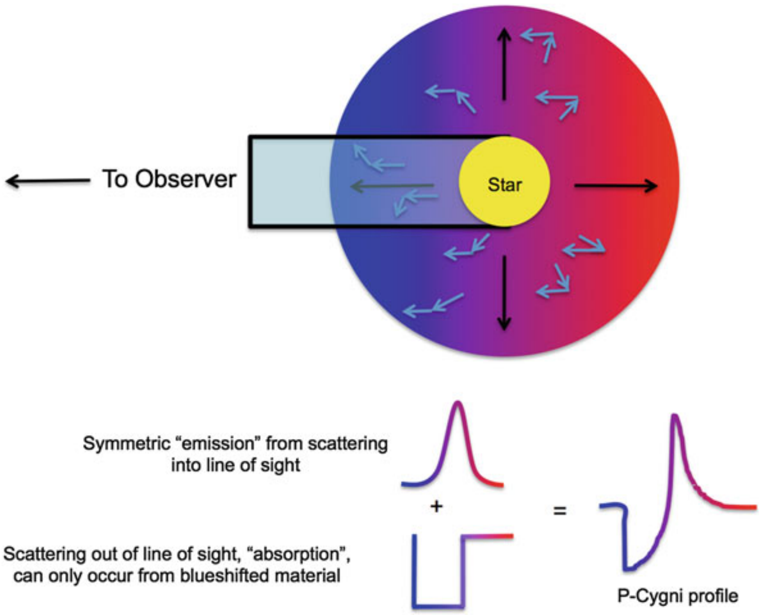

Fig. 2.1 Diagram showing how an expanding envelope or wind presenting significant line opacity around a continuum source leads to the formation of P-Cygni profiles. The *black arrows* denote the outflow direction and the *blue arrows* typical scattering interactions

years on understanding and modelling these UV features (e.g. Drew and Verbunt 1985; Mauche and Raymond 1987; Shlosman and Vitello 1993; Knigge et al. 1995, 1997; Knigge and Drew 1997; Long and Knigge 2002; Noebauer et al. 2010; Puebla et al. 2011). The basic picture emerging from these efforts is of a slowly accelerating, moderately collimated bipolar outflow that carries away $\simeq 1-10\%$ of the accreting material. State-of-the-art simulations of line formation in this type of disc wind can produce UV line profiles that are remarkably similar to observations, as shown in Fig. 2.3.

Much less is known about the effect of these outflows on the optical spectra of high-state CVs. Direct evidence of wind-formed lines comes from isolated observations of P-Cygni-like line profiles in Hα and He I 5876 Å, (Patterson et al. 1996; Ringwald and Naylor 1998; Kafka and Honeycutt 2004). However, the effect of a wind on the *emission* lines in the optical spectrum is unclear. Murray and Chiang (1996, 1997) have shown that the presence of disc winds may offer a natural explanation for the single-peaked optical emission lines in high-state CVs, since they can strongly affect the radiative transfer of line photons (Fig. 2.4; also see Flohic et al. 2012). Stronger support for a significant wind contribution to the optical emission lines comes from observations of eclipsing systems. There, the single-peaked lines are often only weakly eclipsed, and a significant fraction of the line flux remains visible even near mid-eclipse (e.g. Baptista et al. 2000; Groot et al. 2004). This points to

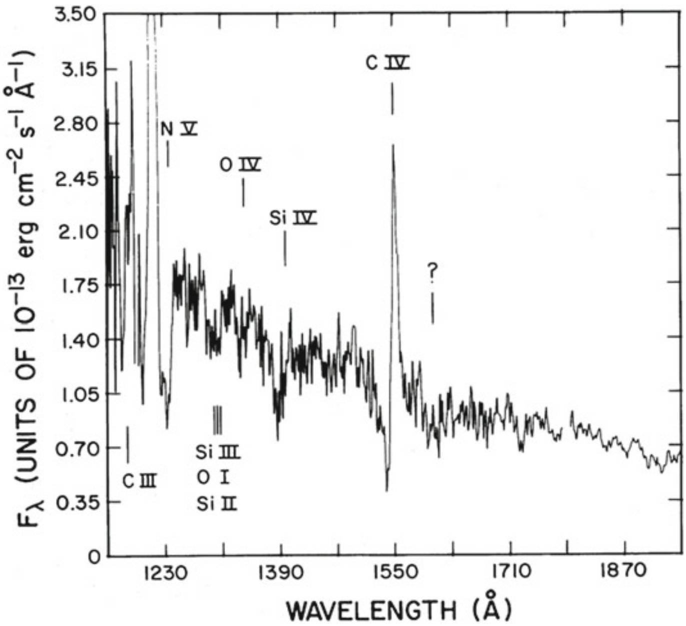

Fig. 2.2 UV spectrum of the DN TW Vir during outburst. The P-Cygni profiles can be seen clearly, demonstrating that a strong, fast outflow is present in the system. *Credit* Cordova and Mason (1982). Copyright AAS. Reproduced with permission

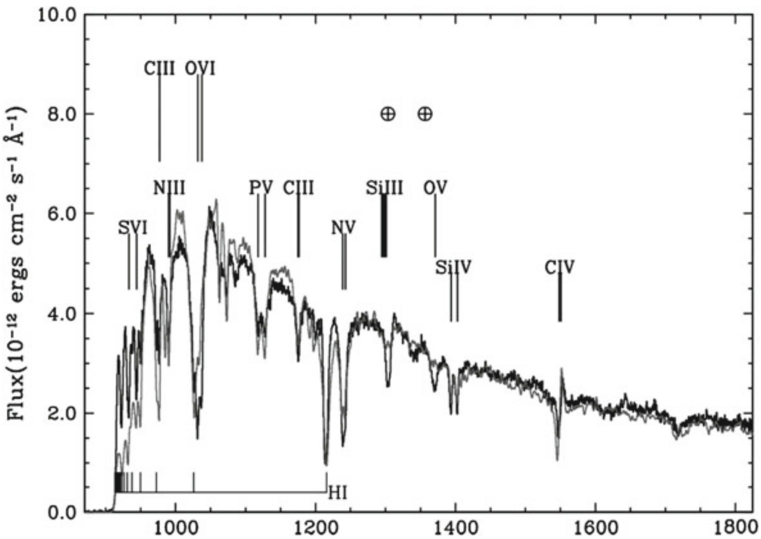

Fig. 2.3 UV spectrum of Z Cam (*black*), compared to a synthetic spectrum from MCRT simulations (*grey*). *Credit* Long and Knigge (2002). Copyright AAS. Reproduced with permission

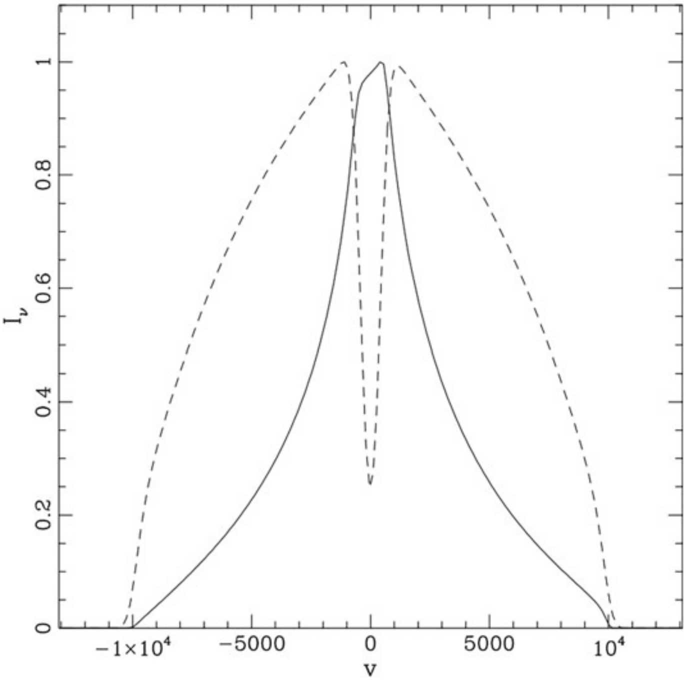

Fig. 2.4 A comparison between a line profile, normalised to have peak intensity of 1, produced from a Keplerian disk (*solid line*) and the same model with an additional disc wind (*dashed line*). The radial velocity component of the disc wind modifies the escape probabilities across the disc, causing a single-peaked line to form. *Credit* Murray and Chiang (1997)

line formation in a spatially extended region, such as a disc wind. It is also possible that a wind may affect the continuum emission of CVs, as described in Sect. 1.4. The effect of an accretion disc wind on the optical line and continuum emission of CVs is addressed directly in Chap. 4.

2.1.2 X-Ray Binaries

As in CVs, evidence for fast outflows in LMXBs is not constrained to a single waveband. UV absorption in outflows was detected when Ioannou et al. (2003) observed C IV 1550 Å P-Cygni profiles with blueshifts of $\sim$1500 km s^{-1} in the LMXB X2127+119. A series of studies also found X-ray absorption features in similar objects (Ueda et al. 1998; Kotani et al. 2000; Parmar et al. 2002). These absorption features appeared to be preferentially detected in 'dipping' LMXBs. Dips in X-ray flux are thought to occur in systems with inclinations $\gtrsim$70° (van der Hooft et al. 1998; Tanaka et al. 2003; Church et al. 2005), and possible explanations involve

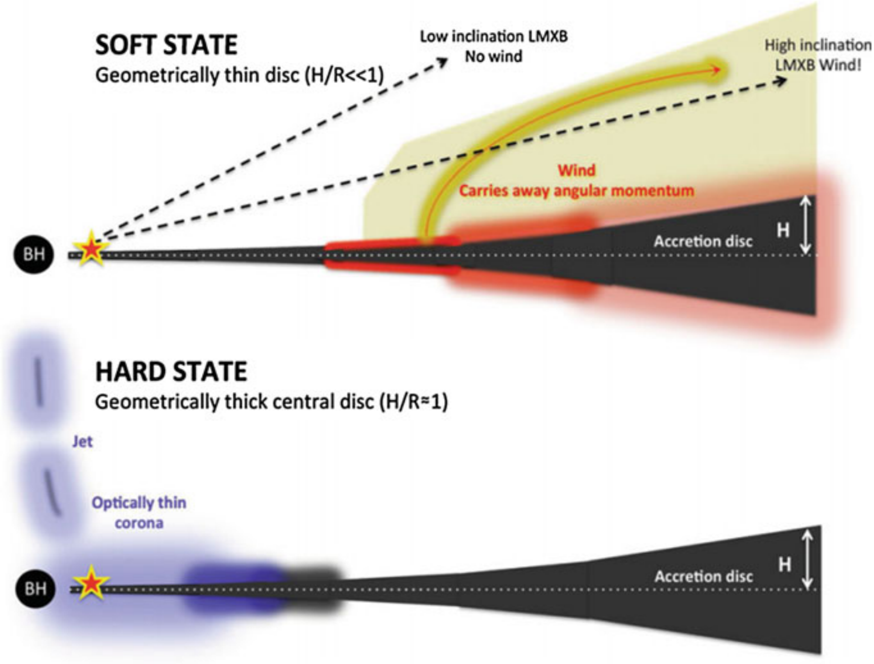

Fig. 2.5 A cartoon illustrating the expected geometry of the disc and outflows in LMXBs in the soft and hard states. *Credit* Fig. 3, Ponti et al. 2012, "Ubiquitous equatorial accretion disc winds in black hole soft states", MNRAS letters, 422, 11

disc precession (Barnard et al. 2006; Shaw et al. 2013), failed state transitions (Soleri et al. 2013; Shaw et al. 2016) or low ionization material partially covering the X-ray source (Tanaka et al. 2003). Ponti et al. (2012) confirmed that broad absorption in highly ionized Fe lines occurred only in the dipping LMXBs in their sample and proposed an equatorial outflow geometry based on this association (see Fig. 2.5). The same study also demonstrated that the winds only appeared in the soft, disc dominated accretion state, on the opposite side of the HID to the region where jets are common (Fig. 2.6). This exciting result illustrates how important winds are to our understanding of accretion and requires that we expand the discussion of accretion states from 'disc-jet' coupling to also include winds.

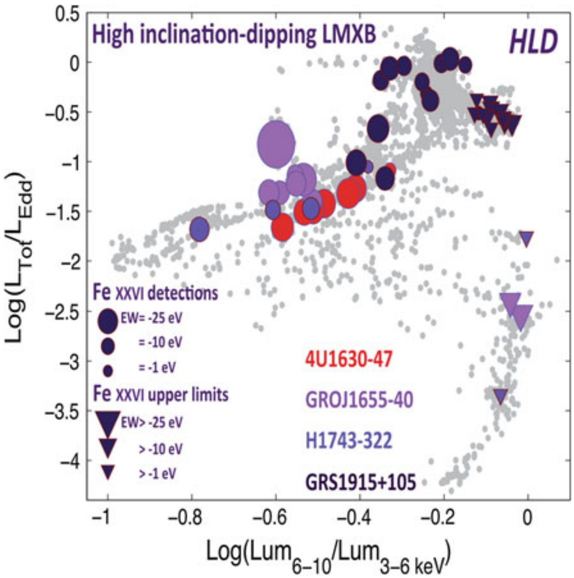

Fig. 2.6 Hardness-luminosity diagram for four dipping LMXBs, demonstrating that winds appear only in the soft state. The points are colour-coded by system, and are shown against the background *grey* points of all LMXBs studied by Ponti et al. 2012. None of the low inclination sources in their sample show Fe XXVI absorption detections. *Credit* Fig. 2, Ponti et al. 2012, *"Ubiquitous equatorial accretion disc winds in black hole soft states", MNRAS letters, 422, 11*

2.1.3 AGN and Quasars

2.1.3.1 Broad Absorption Line Quasars

Perhaps the clearest evidence of outflows in AGN is provided by the blueshifted (∼0.1c) ultraviolet BALs seen in approximately 20% of quasars (Weymann et al. 1991; Knigge et al. 2008; Dai et al. 2008; Allen et al. 2011). High-ionization BAL quasars (HiBALs) only show broad, blue-shifted absorption in species such as C IV, Si IV, N V and O VI, the most prominent BAL profile often being associated with the C IV 1550 Å line. In addition to the more common HiBALs, approximately 10% of BALQSOs also show absorption in lower ionization species such as Mg II and Al III (LoBALs; Voit et al. 1993; Gibson et al. 2009); an even smaller subset also show absorption in Fe II and III (FeLoBALs; Becker et al. 2000; Hall et al. 2002). Some example spectra of BAL quasars from the HST and SDSS archives are shown in Fig. 2.7, with important spectral lines marked.

The simplest explanation for the incidence of BAL quasars (BALQSOs) is in terms of an accretion disc wind viewed from different angles. This principle of geometric unification is very similar to the idea behind the UP95 and AM95 models discussed in Chap. 1. According to this paradigm, a biconical wind rises from the accretion disc so that the BALQSO fraction is associated with the covering factor of the outflow. This fraction has been estimated by various authors using different selection criteria, with values ranging between 10 and 40% depending on the treatment of selection effects and the classification scheme used (Weymann et al. 1991; Trump et al. 2006; Knigge et al. 2008; Dai et al. 2008; Allen et al. 2011).

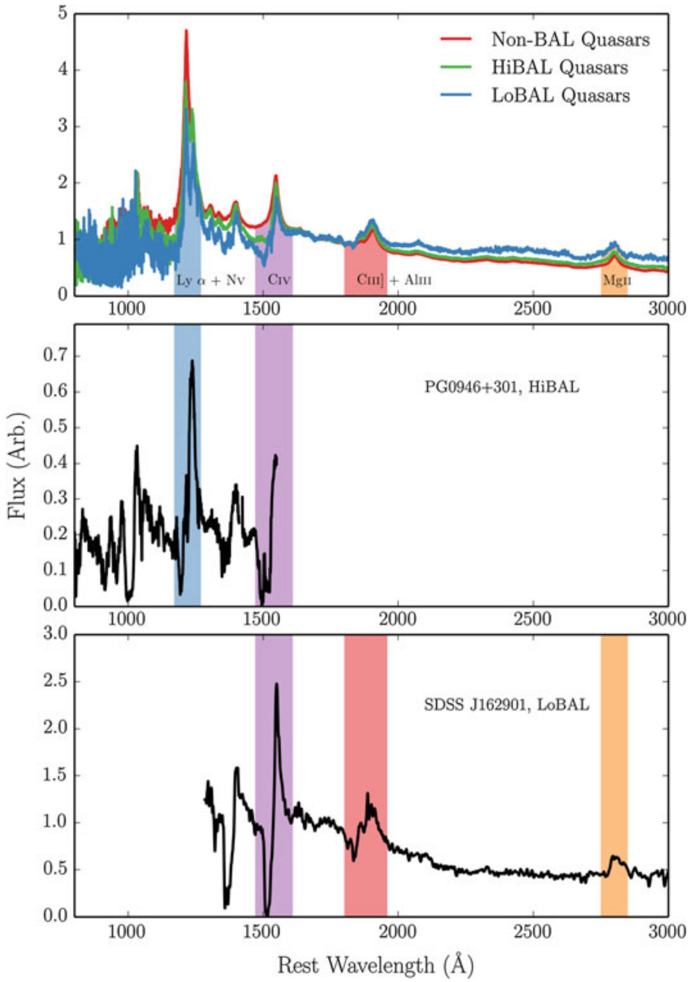

Fig. 2.7 *Top panel* A comparison between the SDSS non-BAL, HiBAL and LoBAL composite spectra as presented in Reichard et al. (2003). *Bottom two panels* Two individual examples of a HiBAL and LoBAL quasar spectrum, respectively. In all panels some of the more prominent lines are labeled and shaded, and the object name is given in the *bottom two plots*

BAL quasars can also be interpreted in an *evolutionary* context, in which quasars spend a certain proportion of their life in the 'BAL phase'. Models generally put this phase near the start of the quasar lifetime (Hazard et al. 1984; Surdej and Hutsemékers 1987; Boroson and Meyers 1992; Zubovas and King 2013), after a dust-enshrouded phase, but before the main quasar period. It is perhaps more likely that *both* evolutionary and geometric effects are at work (Borguet and Hutsemekers 2010; Dai et al. 2012). One of the main problems with testing these two paradigms is that many of the properties of BAL quasars fit naturally into either picture, and so disentangling their true nature is challenging. The latter chapters of this thesis attempt to address this issue by testing the geometric unification model and seeing how close this simple picture can get to explaining the BAL phenomenon.

The BAL fraction, f_{BAL}, is a very useful number and must be at least related to the covering factor of the outflow. However, selection effects associated with the reduction in flux by the BALs themselves (Knigge et al. 2008) and enhanced reddening/extinction in BALQSOs (Reichard et al. 2003; Allen et al. 2011) could lead to significant underestimates of f_{BAL}. The angular dependence of the continuum causes further problems, as objects viewed from higher inclinations could be severely under-represented in a flux-limited sample (Goodrich 1997; Krolik and Voit 1998). Unfortunately, accurately correcting for these effects is difficult. The degree of collimation of the BAL wind is also not well known. Polarisation studies suggest that the wind is roughly equatorial (Goodrich and Miller 1995; Cohen et al. 1995), as also found from hydrodynamical and radiative transfer simulations (Proga et al. 2000; Proga and Kallman 2004; Higginbottom et al. 2013; Borguet and Hutsemékers 2010). However, there is also evidence for polar BAL outflows in radio-loud (RL) sources (Zhou et al. 2006; Ghosh and Punsly 2007). In addition to these uncertainties, the physical scale of the BAL phenomenon is also disputed and may vary from object to object. A common assumption is that the BAL region is roughly co-spatial with the BLR, which is reasonable considering the similar velocity widths and ionization states in BELs and BALs. In this case, the radius of the absorbing material can be estimated as $\sim 100-1000\ r_G$ from reverberation mapping and microlensing (e.g., for BLRs in BALQSOs, Sluse et al. 2015; O'Dowd et al. 2015). However, distances of ~0.1pc ($\sim 10^4\ r_G$) have been estimated in at least some objects from photoionization modelling, conducted using densities calculated from absorption line doublets (Borguet et al. 2013; Chamberlain et al. 2015).

BAL quasars display a wide variety of different trough shapes. The line profiles themselves often show complex structure (Foltz et al. 1987; Ganguly et al. 2006; Simon and Hamann 2010) and can be time variable (Hall et al. 2011; Capellupo et al. 2011, 2012, 2014; Filiz Ak et al. 2012). Furthermore, a subset of quasars show BAL-like absorption troughs with much smaller velocity widths. Depending on their width, these are known as narrow absorption lines (NALs) or 'mini-BALs' (Misawa et al. 2007, 2008; Nestor et al. 2008). While some of this behaviour can be explained once again as a viewing angle effect (e.g. Ganguly et al. 2001), the BAL profile variety and variability implies that BALQSOs are far from a homogenous population, and perhaps suggests the existence of dense substructures (clumps) in their flows. Such clumpiness has been invoked in several disc wind unification models for AGN and quasars (see Sect. 2.3).

The X-ray properties of BAL quasars are particularly important due to the strong ionizing potential of the X-ray radiation. Observationally, BALQSOs are X-ray weak when compared to non-BAL quasars (Gibson et al. 2009). This X-ray weakness is often attributed to the presence of absorbing material with column densities of $N_H \sim 10^{22-24}$ cm^{-2} along the line of sight (Gallagher et al. 1999, 2002; Green et al. 2001; Grupe et al. 2003a; Stalin et al. 2011), although there is also evidence that BALQSOs are *intrinsically* X-ray weak (Sabra and Hamann 2001; Clavel et al. 2006; Morabito et al. 2013). The X-ray properties of BAL quasars are fundamentally coupled to the properties of the wind—the X-ray absorption may, in fact, be caused by the outflow, which in turn has its ionization state determined by the X-ray radiation. Furthermore, the true X-ray luminosities cannot be reliably inferred until the inclinations of BALQSOs are constrained, as gravitational lensing can significantly alter the emergent angular distribution of X-ray emission even for an intrinsically isotropic source (Chen et al. 2013a, b).

Although the observed X-ray emission in BALQSOs is weaker than in otherwise similar quasars, it still still possesses strong ionizing power. This leads to what has become known as the 'over-ionization problem' in BALQSOs: how is the moderate ionization state of the BAL gas maintained in the presence of ionizing X-rays? A number of potential solutions have been proposed, which can be broadly separated into 'shielding' models (Murray et al. 1995; Proga and Kallman 2004) and 'clumpy' models (de Kool and Begelman 1995; Hamann et al. 2013). Some of these models are discussed further in Sect. 2.3 and Chap. 5.

2.1.3.2 Warm Absorbers

Warm absorbers (WAs) are regions of photoionized plasma responsible for some of the characteristic absorption features seen in the soft X-ray spectra of AGN (Reynolds and Fabian 1995). In particular, they produce photoelectric continuum absorption (e.g. Halpern 1984; Cappi et al. 1996; Kriss et al. 1996) and a series of narrow absorption lines in H-like and He-like ions of C, N, O, Si, Ne, and Fe (Kaastra et al. 2000). A wind origin is a common hypothesis for WAs (e.g. Krolik and Kriss 2001). Clear evidence for this comes from the measured blueshifts of the lines, typically on the order of a few 100 km s^{-1} (e.g. Kaastra et al. 2000). X-ray absorption and WAs are often variable (Fabian et al. 1994; Otani et al. 1996), which may be interpreted in terms of the changing kinematics of an accretion disc wind (Connolly et al. 2014). There is also evidence of contemporary and associated UV and X-ray absorption in NGC 5548 (Kaastra et al. 2014) and in mini-BALS (Giustini et al. 2011), and, as mentioned above, BALQSOs often show strong X-ray absorption. A number of other AGN also show simultaneous absorption in their X-ray and UV spectra (e.g. Crenshaw et al. 2003; Crenshaw and Kraemer 2012), although can often arise from absorbers that are not directly associated. Overall, there is evidence that the same outflow may produce observational signatures across a large range of ionization states and line energies.

Some WAs can be modelled well with single absorbers (Kaastra et al. 2000), but most require multiple absorption components with different ionization states (e.g. Kriss et al. 1996; Orr et al. 1997; Krolik and Kriss 2001; Connolly et al. 2014). One common way to parameterise the ionization state of a plasma is via an ionization parameter proportional to the ionizing luminosity, given by (e.g. Reynolds and Fabian 1995)

$$\xi = \frac{L_H}{n_H R^2}, \tag{2.1}$$

where L_H is the luminosity above 13.6eV, and n_H is the number density of H atoms. If the absorber is stratified and the SED subject to absorption, self-consistent ionization and radiative transfer models should really be used to model the spectrum (see e.g. Chap. 3). This is because optically thin ionization parameter estimates will not properly capture the ionization physics due to the variation of the SED shape within the medium. The overall body of observations points towards an outflow with a stratified ionization structure ranging from $\log(\xi/\text{erg s}^{-1}\text{ cm}) \sim$0–2 and densities on the order of 10^7 cm^{-3}, located at around $\sim 10^{16}$ cm. These physical conditions or scales are not well constrained, and the connection to other outflows, such as the ultra-fast outflows introduced in the next section, is unknown. Timing observations may help to shed light on the properties of the mysterious, but ubiquitous, AGN WAs (Silva et al. 2015).

2.1.3.3 Ultra-Fast Outflows

In addition to acting as WAs, winds can also imprint clear absorption features in highly ionized Fe Kα lines in AGN such as PDS 456 (Reeves et al. 2003; Gofford et al. 2014; Matzeu et al. 2016), MCG-5-23-16 (Braito et al. 2007) and PG 1211+143 (Pounds and Reeves 2009; Fukumura et al. 2015). These outflow signatures are fairly common in Seyfert galaxies (Tombesi et al. 2010; Gofford et al. 2013). One example of such a feature is shown in Fig. 2.8, along with a simple spherical outflow model fit (Nardini et al. 2015). The high velocities ($\sim$0.1c) inferred from the line blueshifts have lead to these winds becoming known as ultra-fast outflows, or UFOs.

UFO are characterised by ionization parameters in the range $\log(\xi/\text{erg s}^{-1}\text{ cm}) \sim 3 - 4$ and column densities $N_H > 10^{22}$ cm^{-2}. Their high mass-loss rates and large energy budgets mean that they are natural candidates for AGN feedback (see Sect. 2.5). Measurements of their kinetic luminosities suggest that UFOs have sufficient energy to affect their host galaxy (Gofford et al. 2015). In fact, a large-scale molecular outflow has recently been detected in one UFO host, possibly driven by the UFO itself (Tombesi et al. 2015). As with WAs, many of the models used to constrain physical parameters are simplistic, and assume single ionization parameters, large covering factors and thin expanding shells of outflow. Under the assumption of a thin expanding shell, the mass-loss rate can be estimated using (e.g. Borguet et al. 2012)

$$\dot{M}_W \sim \Omega \mu N_H m_p v_{\text{out}} R_{\text{out}}, \tag{2.2}$$

where Ω is the solid angle covered by the outflow, N_H is the column density, m_p is the proton mass, μ is the mean molecular weight, v_{out} is the outflow velocity and R_{out} is the radius of the shell, often approximated as the launch radius of the outflow. In reality, the absorber is probably much more complex, and full RT and photoionization simulations are required to accurately model the expected spectrum. In a series of papers, Sim et al. (2008, 2010a, b) carried out such calculations and found that reasonable verisimilitude with Fe line profiles could be achieved. However, as with many models of AGN, a holistic, broad wavelength range fit is still required.

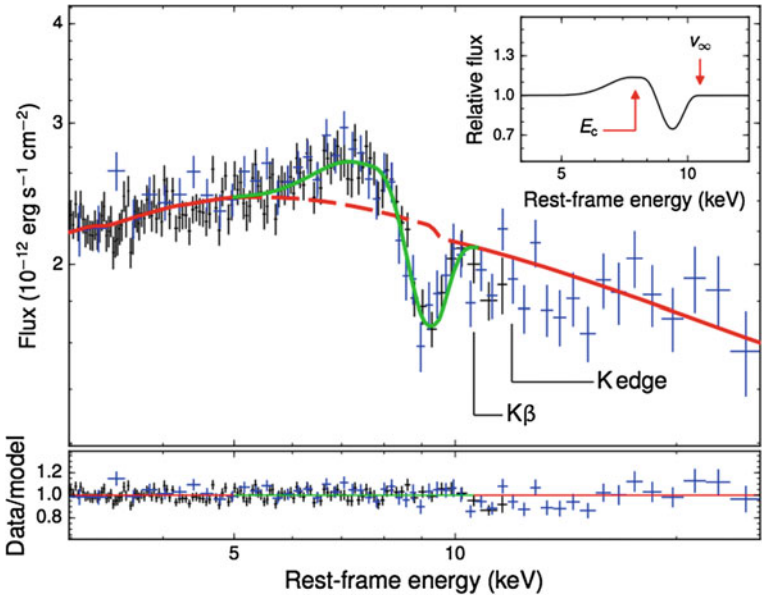

Fig. 2.8 X-ray spectrum of PDS 456 fitted with a P-Cygni profile from a spherical outflow model. *XMM-Newton* data is shown in *black* with two combined *NuStar* observations in *blue*. *Credit* Figure 3, Nardini et al. (2015), Science, 347, 860. Reprinted with permission from AAAS

2.1.4 Stellar Winds

Although stellar winds are clearly not accretion disc winds, they provide a useful, and better understood, testing ground for much of the physics of radiatively-driven outflows. Wolf-Rayet (WR) stars and O-stars possess strong outflows with mass-loss rates of up to $10^{-5}\ M_\odot\ \mathrm{yr}^{-1}$, thought to be driven by radiation pressure mediated by spectral lines (see Sect. 2.2.3). Over the typical lifetime of a massive star ($\sim 10^6$ year), this can have a significant impact on the overall stellar mass, causing losses of around $10\ M_\odot$ of material.

As with the systems described previously, the P-Cygni profiles seen in hot, massive stars provide the key evidence for the presence of a strong wind (see Fig. 2.9). Mass-loaded winds are also thought to be responsible for the emission lines seen in hot star spectra (e.g. Pauldrach et al. 1994). Indeed, emission line diagnostics have been particularly important in determining the mass-loss rates of stellar winds and have also been used to demonstrate that line-driven stellar winds are clumpy.

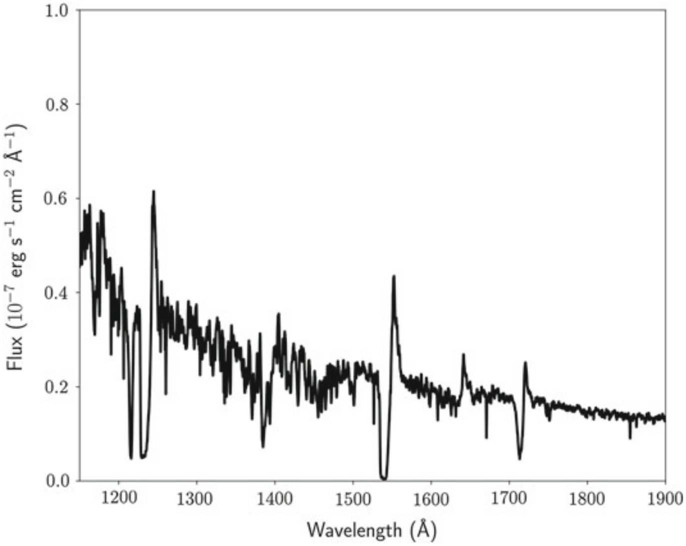

Fig. 2.9 UV spectrum of one of the brightest massive O stars, the O4 supergiant ζ Puppis. The spectrum is obtained from IUE UV observations

2.1.4.1 Clumping in Stellar Winds

Evidence for clumping in hot star winds comes from a range of sources. Perhaps the most conclusive is from electron scattering wings in emission lines: homogenous models overestimate the strength of these wings, whereas clumpy models produce good agreement with data (Hillier 1984, 1991; Hamann et al. 1992, 1994; Schmutz 1997). Further evidence for clumping comes from line variability (Prinja and Smith 1992) and polarisation (Brown et al. 1995). Clumping is theoretically expected in line-driven winds (see Sect. 2.2.3 and the review by Owocki 2014) and is directly dealt with in this thesis. In Chap. 5, I describe the treatment of clumping I have implemented in our radiative transfer code, before presenting results from a clumpy AGN wind model.

2.1.5 Outflow Physics

The spectra in Figs. 2.2, 2.7 and 2.9 show striking similarities—characteristic broad, P-Cygni-like absorption features in UV resonance lines extending to high blueward velocities—despite vast differences in mass and scale. Furthermore, some of the phenomena observed in e.g. stellar winds may naturally solve some of the unanswered questions in other systems. For example, clumping may prevent over-ionization in AGN outflows. It would seem that at least some of the physics of outflows, like accretion physics, is universal, and that lessons learned from smaller-scale systems may be scaleable to AGN and quasars. In order to understand if the similarity extends beyond a cosmetic one, I will discuss some of the underlying physical mechanisms that may be responsible for accelerating these outflows.

2.2 Driving Mechanisms

Let us consider a parcel of ideal gas. By imposing nothing more than conservation of mass, energy and momentum on that parcel, and using Maxwell's equations, we can write down three equations of magnetohydrodynamics (MHD):

$$\frac{D\rho}{Dt} + \rho\nabla \cdot \vec{v} = 0, \tag{2.3}$$

$$\rho\frac{Dv}{Dt} = -\nabla P + \frac{1}{4\pi}(\nabla \times \vec{B}) \times \vec{B} + \rho\vec{g}_{rad} + \rho\vec{g}, \tag{2.4}$$

$$\rho\frac{D}{Dt}\left(\frac{u}{\rho}\right) = P(\nabla \cdot \vec{v}) + \rho\mathcal{L}. \tag{2.5}$$

Here, D denotes a derivative within the comoving frame of the gas parcel, $\vec{v}$ is the velocity, ρ is the gas density, $\vec{B}$ is the local magnetic field, $\vec{g}_{rad}$ is the radiation force per unit mass, $\mathcal{L}$ is the cooling rate of the gas, u is the energy density and $\vec{g}$ denotes the gravitational acceleration vector.

Equation 2.3 is the *continuity equation* and describes conservation of mass. Equation 2.4 is the *equation of motion* and describes conservation of momentum. Equation 2.5 is the *equation of energy conservation*. Equation 2.4 can be used to neatly demonstrate how an outflow can be driven. I have deliberately written Eq. 2.4 so that all the force terms lie on the RHS. For an outflow to be driven from an accreting object, one of the terms on the RHS must dominate over gravity, $\rho\vec{g}$. These terms thus signify three potential driving mechanisms.

- Magnetic/Lorentz Forces, $\frac{1}{4\pi}(\nabla \times \vec{B}) \times \vec{B}$.
- Radiative Forces, $\rho\vec{g}_{rad}$.
- Thermal Pressure, $-\nabla P$.

We can now examine under what physical conditions (and in which corresponding astrophysical objects) we might expect these forces to overcome gravity and cause a parcel of mass to escape to infinity. In other words: *what might drive a wind?*

2.2.1 Thermal Winds

In a disc in hydrostatic equilibrium (HSE), thermal pressure balances gravity in the vertical direction. The equation of motion in this z direction can then be written as

$$\rho \frac{Dv_z}{Dt} = -\frac{\partial P}{\partial z} + \rho g_z = 0. \tag{2.6}$$

Clearly, if the thermal pressure is significantly increased, this equilibrium condition no longer holds. This can occur in accretion discs at temperatures in excess of $\sim 10^7$ K—where other forces are negligible compared to thermal pressure—and where the escape velocities are relatively low (i.e. far out in the disc). Due to the temperature and gravity scalings, this means that XRBs are natural candidates for showing evidence of thermally driven winds. The outer disc can be heated to the Compton temperature by the central X-ray source, potentially driving relatively high mass-loss rate outflows (Begelman et al. 1983; Woods et al. 1996). This driving mechanism has been proposed as a natural explanation for the ever-present equatorial outflows in soft state XRBs (Ponti et al. 2012). However, they are much less likely candidates in CVs and AGN, because there the escape velocity tends to greatly exceed the thermal velocity.

2.2.2 Radiatively Driven Winds

Under spherical symmetry and for opacities dominated by electron scattering, one simply obtains the Eddington limit discussed in Sect. 1.1.1 when $\rho \vec{g}_{rad} = \rho \vec{g}$. Hence, sources must be fairly close to the Eddington luminosity in order to drive an outflow purely from radiation pressure on electrons. There are a number of accreting systems that may drive super-Eddington (or close to Eddington) outflows, such as AGN with UFOs (e.g. Reeves et al. 2002; Pounds et al. 2016), NLSIs (Done and Jin 2015) and ultra-luminous X-ray sources (ULXs; Walton et al. 2013). However, high-state CVs are significantly below the Eddington limit (Warner 2003), and at least some BALQSOs have low Eddington fractions ($\sim$25% have $L/L_{\rm Edd} < 0.1$; Grupe and Nousek 2015). These systems may nevertheless be capable of radiatively driving strong outflows due to the influence of line opacity.

2.2.3 Line-Driven Winds

Under spectra do not, in general the right ionization conditions, radiation pressure mediated by spectral lines can be a significant acceleration term in a partially ionized plasma (Castor et al. 1975, hereafter CAK). The most common way to parameterise the cumulative effect of lines on the radiation force is via the *CAK force multiplier*, $\mathcal{M}(t)$, which modifies the equation for the acceleration due to radiation pressure on electrons to give (Castor 1974 CAK)

$$\vec{g}_{rad} = \frac{\sigma_T F}{\mu c m_p} \mathcal{M}(t), \tag{2.7}$$

where F is the flux, and μ is the mean atomic weight. $\mathcal{M}(t)$ can be approximated by (Abbott 1982)

$$\mathcal{M}(t) = k\, t^{-\alpha} \left(\frac{n_e}{10^{11}\ \mathrm{cm}^{-3}} \right)^{\delta}. \tag{2.8}$$

Here, k, α and δ are parameters with best-fit values of 0.28, 0.56 and 0.09, respectively, in O-star winds (Abbott 1982), and v_i is the component of the velocity field in the direction being considered. This is normally a line between the source of radiation and any given location in the wind. The dimensionless optical depth, t, is given by

$$t = \frac{\sigma_T \rho v_{th}}{m_p |d(v_i)/ds|}, \tag{2.9}$$

where v_{th} is the thermal speed, ρ is the density, and $d(v_i)/ds$ represents the derivative of v_i along the same direction it has been defined. It is possible to show (CAK, Owocki et al. 1988) that the maximum force multiplier, $\mathcal{M}_{\max}(t)$, is around 2000–4000. This is already an interesting result, as it tells us that line-driven outflows can be accelerated when accretion rates/luminosities are much lower than the Eddington limit. Indeed, using Eq. 2.7 we can see that a radiatively driven wind can be accelerated when $L > L_{\mathrm{Edd}}/M(t)$, where $M(t)$ will depend in detail on the spectral lines in question and their relative ionization and excitation fractions. Line-driven winds are present in O-stars and Wolf-Rayet stars, and the theory produces good matches with observations (e.g. Friend and Abbott 1986; Pauldrach et al. 1986, 1994; Hamann et al. 2008). It is also a strong candidate for driving the winds seen in high-state CVs when the accretion disc is UV bright (Pereyra et al. 1997; Proga et al. 1998; Proga 2005, see also Sect. 2.3.4).

Line driving may be a promising mechanism to explain BAL outflows as well, since the strong UV resonance lines seen in absorption in O stars are also present in BALQSOs. The presence of 'line-locked' features (Bowler et al. 2014) and the 'ghost of Lyα' (Arav et al. 1995; Arav 1996; North et al. 2006) in the spectra of some BALQSOs also suggests that line-driving is at least contributing to the acceleration of the wind (but see also Cottis et al. 2010). However, the presence of an X-ray source complicates matters. I have already briefly touched on the 'over-ionization' problem in AGN outflows, but it now has another consequence. Not only will strong X-rays prevent the right features forming in the spectrum, but, if the outflow is line-driven, they may prevent the wind existing in the first place. Despite these problems, some hydrodynamic simulations of line-driven AGN winds have been successful in producing high mass-loss rates (see Sect. 2.3.4).

Line-driving is subject to a strong instability known as the line deshadowing instability (LDI; Lucy and Solomon 1970; MacGregor et al. 1979; Owocki and Rybicki 1984, 1985). The basic idea is that any velocity perturbation in a line-driven flow can cause a 'deshadowing' effect, as the fluid element will now be in resonance with a region of the spectrum that is less absorbed. Thus, an increase in the line force will occur in proportion with this velocity perturbation, and the instability can grow. Time-dependent numerical modelling of the LDI has shown that it can produce a clumpy flow (Owocki et al. 1988; Feldmeier 1995; Šurlan et al. 2012; Owocki 2014) that may explain the observational characteristics of clumping in stellar winds (see Sect. 2.1.4.1). The LDI is also of interest in CV and AGN winds, as it may affect the ionization state of the flow and possibly the inferred mass-loss rates.

2.2.4 Magnetic Winds

There is still great uncertainty over the magnetic fields in accretion discs and the physics of these magnetic processes. However, the MRI is one of the leading candidates for explaining angular momentum transport in accretion discs, implying that magnetic processes are important in their dynamics. Thus, in many senses, magnetic driving is an attractive wind driving mechanism. There are two main ways in which magnetic forces can drive an accretion disc wind, which are best explained by writing down an alternative form for the Lorentz force,

$$\vec{F}_m = \frac{1}{4\pi}(\nabla \cdot \vec{B})\vec{B} - \nabla \frac{B^2}{8\pi}, \tag{2.10}$$

where $B = |\vec{B}|$. The first term can be thought of as a magnetic *tension* associated with the field lines and the second as an isotropic magnetic *pressure*.

Historically, the most popular magnetic wind model has been the 'bead on a wire' mechanism proposed by Blandford and Payne (1982) and Pelletier and Pudritz (1992). In these models, the poloidal magnetic field is dominant and is anchored in the accretion disc. A wind can then be driven by magnetic tension, as the first term in the above equation operates on fluid elements ('beads') on the surface of the accretion disc. This can accelerate a wind when the poloidal component of the field makes an angle of $>30°$ with the normal to the disc surface. These models are known as magnetocentrifugal winds, as it is the interaction between centrifugal forces and a strong, large-scale, ordered magnetic field threading the disc that drives the wind. Magnetocentrifugal wind models have been proposed for both AGN and YSOs (Pelletier and Pudritz 1992; Konigl and Kartje 1994; Kudoh and Shibata 1997), and numerical simulations have demonstrated that this mechanism can produce jets and outflows (Romanova et al. 1997; Ouyed and Pudritz 1997; Ustyugova et al. 1999).

In an alternative MHD model the isotropic magnetic pressure is responsible for driving the outflow (Proga 2003). In this case the toroidal component dominates over the poloidal component and drives a slow, dense outflow which behaves more like a thermally-driven wind (i.e. it conserves specific angular momentum rather than angular velocity).

2.3 Accretion Disc Wind Models

A number of different wind models have appeared in the literature over the years, each attempting to explain the different observational characteristics of quasars and CVs with a mixture of conceptual frameworks and underlying physics. In AGN and quasars, the authors behind the models attempt to explain the origins of BELs and BALs, although some extend their remit into the infra-red, radio and X-ray regimes. In CVs, the picture is slightly more straightforward, as the geometry of the outflow is better constrained (see Sect. 2.1.1). Below, I will briefly discuss a few examples that have gained traction over the years, particularly those describing quasars and unification, before outlining the kinematic prescription I have used in the modelling that forms part of this thesis. This prescription has been successfully applied to both CVs and AGN.

2.3.1 MCGV95: A Line-Driven Wind Model for AGN

MCGV95 proposed a model in which a smooth wind rises from an accretion disc with a launch radius of around 10^{16} cm. The wind is equatorial, with an opening angle of 5°, and is accelerated by line forces up to a terminal velocity of 0.1c. A sketch of the geometry is shown in Fig. 2.10. One of the key features of the model is the presence of a 'shield' of hitchhiking gas, which protects the outflow from X-ray over-ionization and allows radiation pressure on UV resonance lines to efficiently accelerate the flow.

MCGV95 found that BAL profiles were seen for an observer looking into the wind cone, and significant collisionally excited line *emission* emerged at low inclinations. This line emission came from a relatively small BLR ($r_{BLR} \sim 10^{16}$ cm) at the base

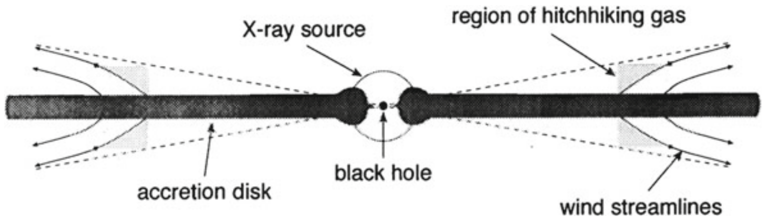

Fig. 2.10 Cartoon showing the geometry of the MCGV95 model. *Credit* Murray et al. 1995. Copyright AAS. Reproduced with permission

of the wind, where densities were high ($n_e \approx 10^{10}$ cm^{-3}). The MCGV95 model was one of the first successful disc-wind unification models. It is especially impressive as it includes photoionization calculations and quantitative estimates of the resultant line EWs. However, the effects of multiple scattering and complex radiative transfer effects could not be included in the calculations (see Chap. 5).

2.3.2 De Kool and Begelman: A Radiatively Driven, Magnetically Confined Wind

It is, of course, possible that radiation and magnetic fields are both important in determining the outflow characteristics. In the de Kool and Begelman (1995) model, radiation pressure drives an outflow from an accretion disc and also compresses the magnetic field lines that are dragged along with the flow. This causes the magnetic field strength in certain regions to be comparable to the gas pressure, meaning that clouds can be magnetically confined in the flow. A diagram is shown in Fig. 2.11. The authors find that such a model would naturally emerge at a fairly equatorial angle with a covering factor of around 10%, and that lower ionization material would be intercepted when the system was viewed from higher inclinations, potentially explaining some of the properties of LoBALQSOs.

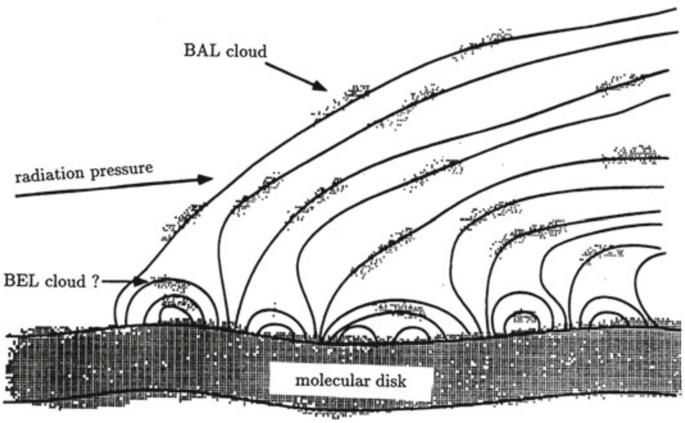

Fig. 2.11 A cartoon showing the components in the De Kool and Begelman model. *Credit* De Kool and Begelman 1995. Copyright AAS. Reproduced with permission

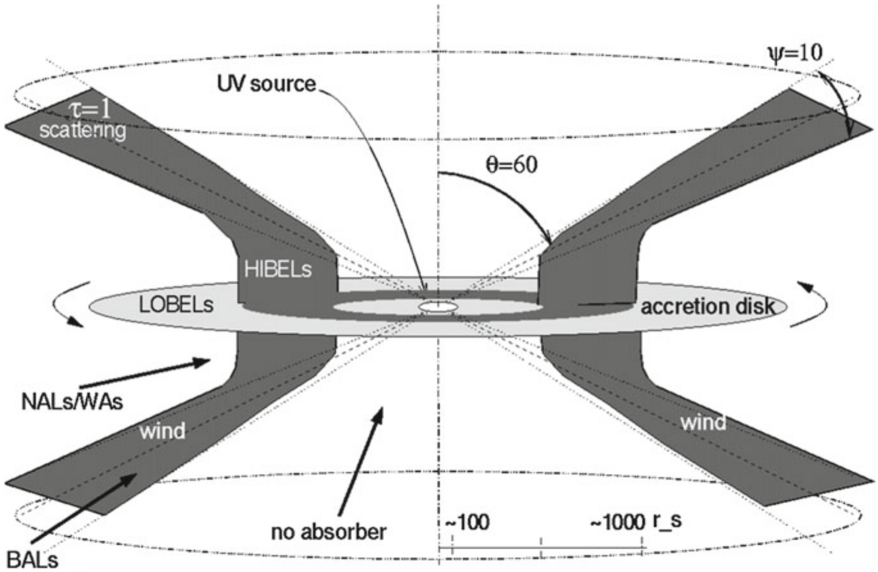

Fig. 2.12 A schematic showing the main features of the Elvis model. A biconical wind rises from an accretion disc, and the observed spectrum is determined purely by the viewing angle of the observer. *Credit* Martin Elvis

2.3.3 Elvis 2000: A Structure for Quasars

Elvis (2000) expanded on the work of MCGV95 by proposing a simple disc wind model, empirically designed to explain as much of quasar phenomenology as possible within one unifying framework. The geometry of Elvis' is shown in Fig. 2.12. As in the two previous models, observers looking into the wind cone will see a BALQSO, whereas observers looking down onto the wind will see a type 1 quasar. Initially, the wind rises vertically, so that observers looking underneath the flow will see NALs, due to the small range of velocities intercepted by their line of sight.

The flow conserves angular momentum, such that the initial Keplerian velocities determine the BEL widths, before accelerating to BAL-like velocities of $\sim$0.1c. The wind is assumed to be two-phase, with BEL and BAL clouds embedded in a warm, highly ionized medium (WHIM). This WHIM is responsible for WA-like absorption and the X-ray scattering phenomena seen in AGN. It is also responsible for confining the BAL and BEL clouds, allowing high densities and cooler temperatures to exist within the flow. The ionization structure for the wind is stratified, such that the material further out along the disc plane is somewhat shielded from the inner disc and X-rays. This allows the lower ionization BEL profiles to form in the right locations, and also means that LoBAL profiles would be seen at a subset of inclinations.

2.3.4 Proga et al.: Line-Driven Hydrodynamic Models for AGN and CVs

Around the turn of the century, Daniel Proga and collaborators published a series of important papers in which they conducted hydrodynamic simulations of line-driven disc winds in AGN and CVs. In the first of these, the problem considered was that of disc winds in CVs (Proga et al. 1998). In their model, the disc was assumed to radiate according to the α-disc model, and the central WD was also included as a radiating source. They found that when the disc has $L/L_{\rm Edd} \gtrsim 1/\mathcal{M}_{\rm max}(t) \approx 0.001$, then strong, line-driven outflows are driven from a few WD radii with bending angles of $\sim$45°. This result agreed qualitatively with outflows in CVs, and later efforts to compute synthetic line profiles produced promising results (Proga et al. 2002a). This was the first successful demonstration of line driving in a full hydrodynamic simulation.

The same principle was then applied to the problem of AGN outflows, with the additional complication of an ionizing X-ray source now included (Proga et al. 2000; Proga and Kallman 2004, hereafter PK04). A snapshot from the PK04 model is shown in Fig. 2.13. An inner 'failed' wind forms in this simulation, which initially rises up from the disc before being over-ionized by the central X-rays. Crucially, this acts as a shield, similarly to the hitchhiking gas proposed by MCGV95, and allows a line-driven wind to be accelerated further out in the disc. This outflow can be seen clearly in Fig. 2.13.

One of the interesting results of these simulations is that they tended to produce somewhat unsteady, clumpy flows. In the CV case, this was caused by the interaction between the line force and gravity, as both force terms vary differently with height. In the AGN case, it was instead due to the critical importance of the ionization state on the line force. Parcels of gas can only be accelerated if they have the 'right' ionization state, and this depends critically on both their density and the radiation field they see. This causes a coupling between the dynamics of the flow and the path of ionizing radiation. The radiation field also helps determine the geometry of the outflow, as increasing the strength of the radiation interior to the launch radius tends to flatten out the wind and lead to more equatorial outflows (Proga et al. 1998; Proga 2005). Indeed, the outflow in the CV case is more collimated than the equatorial AGN outflow for this reason. This is particularly important when considering quasar unification, as it means the viewing angles of BALQSOs can provide information about where the wind is launched. Along with more empirical motivations, the results of this hydrodynamical modelling are one of the reasons for adopting different geometries for the CV and quasar models presented in Chaps. 4 and 5 respectively.

It is worth noting that the smaller scale LDI could not be included in this model, partly for computational reasons and partly because of the approximations used to treat the radiation field. Treating the radiation transport is also important for other reasons. Higginbottom et al. (2014, hereafter H14) showed that, in this particular geometry, multiple scattering actually makes shielding ineffective, and radiation will simply find its way around the failed wind to over-ionize the flow beyond (see also

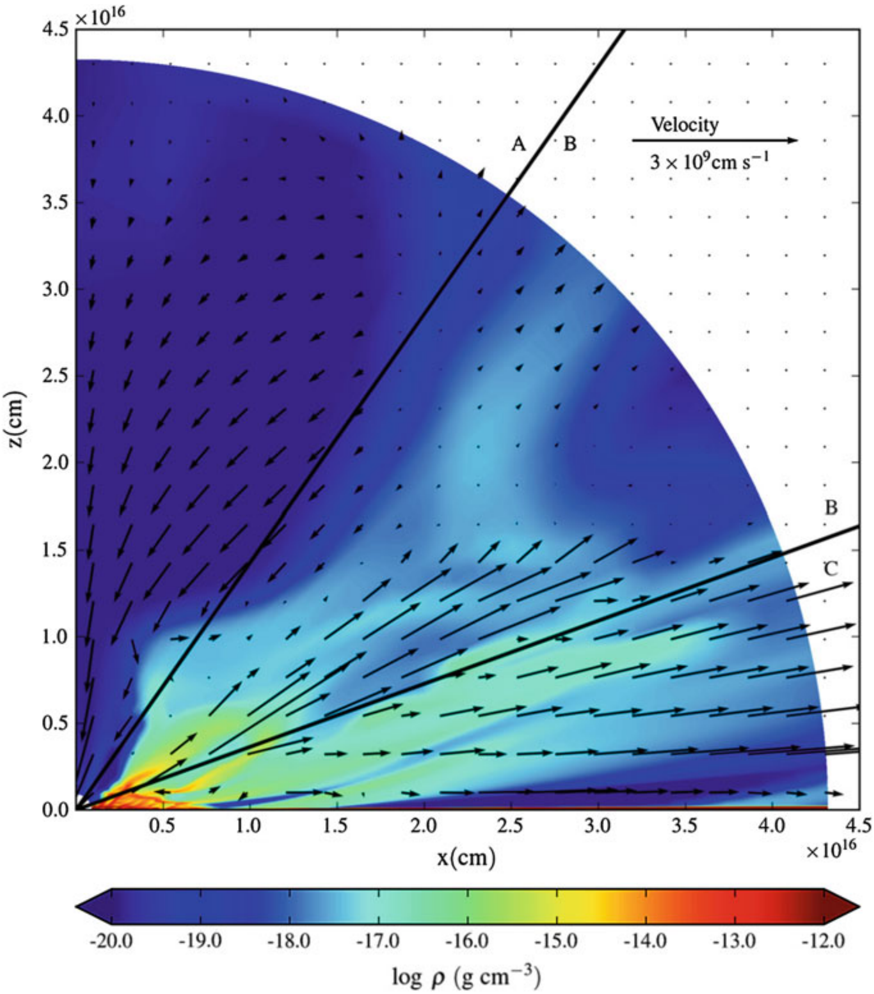

Fig. 2.13 A snapshot of the PK04 model. *Colours* shows the density and arrows show the velocity of the flow. The radial lines separate three areas described by H14. *Credit* Higginbottom et al. (2014). Copyright AAS. Reproduced with permission

Sim et al. 2010b). Ideally, full radiative transfer and hydrodynamical simulations would be used to estimate the viability of line-driven winds. Our team is currently working on this problem (see H14 for the first step); however, much can also be learned from simpler, kinematic prescriptions for outflows, which can already be modelled with full treatments of radiative transfer and ionization.

2.4 A Kinematic Prescription for a Biconical Wind

Shlosman and Vitello (1993, hereafter SV93) expanded on the work of the stellar wind community (e.g. Abbott and Lucy 1985) in proposing a kinematic model for an accretion disc wind. Unlike hydrodynamical models, this model has no real predictive power in terms of velocities and mass-loss rates. Instead, one sets these quantities in advance and examines the resultant properties of the flow and the emergent spectra. The SV93 prescription is the most common way of describing the outflow in the radiative transfer code PYTHON (see Chap. 3) and has been used to simulate spectra for CVs (Long and Knigge 2002; Matthews et al. 2015, Chap. 4), AM CVn systems (Kusterer et al. 2014) and AGN/quasars (Higginbottom et al. 2013; Matthews et al. 2016; Yong et al. 2016, Chap. 5). An alternative description was developed by Knigge et al. (1995) and has been used in similar applications (Long and Knigge 2002; Sim et al. 2008, 2010a), as well as for young-stellar objects (YSOs; Sim et al. 2005). Kinematic prescriptions have thus been a useful tool in allowing quantitative tests of conceptual models, specifically for assessing their ability to reproduce the observed spectra of a variety of astrophysical systems.

In the SV93 parametrization, a smooth, biconical disc wind emanates from the accretion disc between $r_{\rm min}$ and $r_{\rm max}$. A schematic is shown in Fig. 2.14. The covering fraction of the outflow is also controlled by the inner and outer opening angles of the wind, $\theta_{\rm min}$ and $\theta_{\rm max}$, and the launch angle of the other streamlines is given by

$$\theta(r_0) = \theta_{\rm min} + (\theta_{\rm max} - \theta_{\rm min}) \left(\frac{r_0 - r_{\rm min}}{r_{\rm max} - r_{\rm max}} \right)^{\gamma}, \quad (2.11)$$

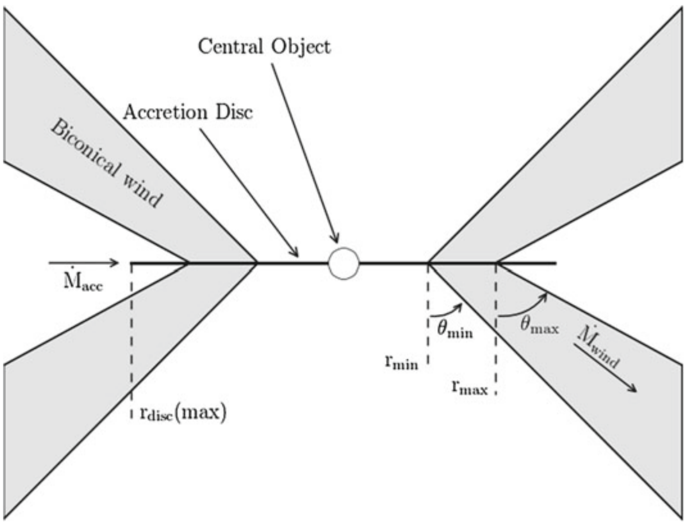

Fig. 2.14 A schematic showing the geometry and kinematics of the SV93 model

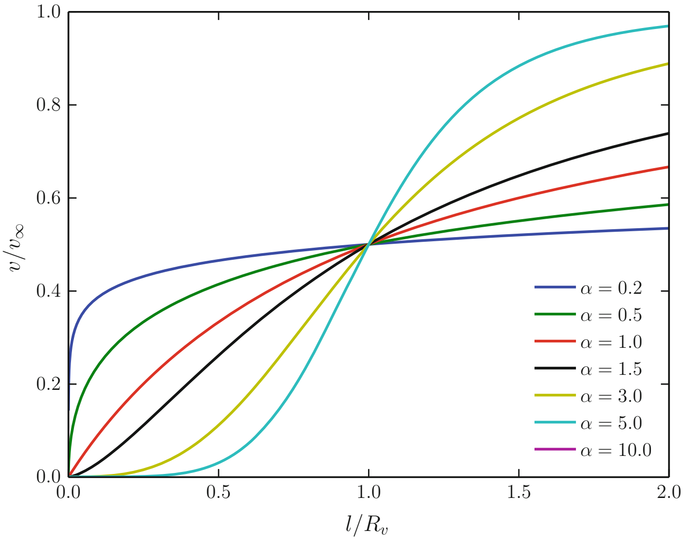

Fig. 2.15 The SV93 velocity law for various values of the acceleration exponent, α

where r_0 is the launch radius of the streamline.

The poloidal (non-rotational) velocity field of the wind, v_l, is given by

$$v_l = v_0 + [v_\infty(r_0) - v_0]\,\frac{(l/R_v)^\alpha}{(l/R_v)^\alpha + 1}, \tag{2.12}$$

where l is the poloidal distance along a particular wind streamline. The terminal velocity along a streamline, v_∞, is set to a fixed multiple of $v_{\rm esc}$, the escape velocity at the launch point. The terminal velocity will therefore be higher for streamlines closer to the inner disc edge. The launch velocity from the disc surface, v_0, is assumed to be constant (set to 6 km s^{-1}). Once the wind is launched, it accelerates, reaching half of its terminal velocity at $l = R_v$. The velocity law exponent, α, controls how quickly the wind accelerates. Larger values of α cause the main region of acceleration to occur close to R_v, whereas smaller values correspond to fast acceleration close to the disc (see Fig. 2.15). The rotational velocity, v_ϕ, is Keplerian at the base of the streamline, and the wind conserves specific angular momentum, such that

$$v_\phi r = v_k r_0, \tag{2.13}$$

where $v_k = (GM_{WD}/r_0)^{1/2}$. The mass-loss rate per unit surface area, $\dot{m}'$, can be controlled by a free parameter, λ_m, such that

$$\dot{m}' \propto \dot{M}_W\, r_0^{\lambda_m} \cos[\theta(r_0)], \tag{2.14}$$

where $\dot{M}_W$ is the total mass loss rate in the wind. This equation is normalised so that when integrated over both sides of the disc the correct $\dot{M}_W$ emerges. I have adopted $\lambda = 0$ throughout this thesis, which corresponds to uniform mass loss across the disc. This could have an effect on the level of shielding present in the flow, and the location of the emission line regions, but should not affect the qualitative conclusions; this is briefly discussed in Sect. 5.4.1. The density at a given point can then be calculated by imposing mass conservation and using the velocity law. At the base of the wind, the density is given by

$$\rho(r_0) = \frac{\dot{m}'(r_0)}{v_z(r_0}. \tag{2.15}$$

At a coordinate (r, z) in the wind, the density is then

$$\rho(r, z) = \frac{r_0}{r}\frac{dr_0}{dr}\frac{\dot{m}'(r_0)}{v_z(r, z)}, \tag{2.16}$$

where the corresponding r_0 is found by considering the streamline that passes through (r, z). These equations govern the kinematics and densities in the wind in the SV93 prescription, which is used extensively throughout this thesis.

2.5 The Big Picture: AGN Feedback

The event horizon of a $10^9\ M_\odot$ BH is approximately 10^{15} cm, a billionth of the radius of a typical galactic bulge. This is roughly the ratio in size between a small coin and the Earth. Even the sphere of gravitational influence of the BH is roughly 1000 times smaller than the size of the galactic bulge. Despite this vast different in scale, there is strong evidence that the physics on the scale of the gravitational radius of the BH affects the evolution and dynamics of its host galaxy. This becomes less surprising when considering the *energetics* of accretion. The binding energy of a galactic bulge, with mass $M_{\rm bulge}$ and velocity dispersion σ_*, is

$$E_{\rm bulge} \approx M_{\rm bulge}\sigma_*^2, \tag{2.17}$$

while the energy released in growing a black hole to a mass M'_{BH} is (Eq. 1.3, assuming $\eta = 0.1$)

$$E_{BH} \approx 0.1 M'_{BH} c^2. \tag{2.18}$$

By combining these two equations, and substituting in typical numbers ($\sigma_* = 0.001c$, $M'_{BH}/M_{\rm bulge} = 10^{-3}$), we can show that

$$\frac{E_{BH}}{E_{\rm bulge}} \approx 10^{-4}\left(\frac{c}{\sigma_*}\right)^2 \sim 10. \tag{2.19}$$

In other words, the energy released when growing a BH can significantly exceed the binding energy of the galactic bulge. This energetic argument is, of course, not sufficient to claim that the accreting BH must affect its host. For example, if the radiated energy never experienced an optical depth of ~ 1, it could not couple to the galactic bulge. However, we have already seen that many outflows in AGN possess kinetic luminosities that are significant compared to the bolometric luminosity. Thus, outflows (and jets) may provide a mechanism by which the vast accretion energies can be transferred to the BH environment.

2.5.1 Observational Evidence for Feedback

Perhaps the most famous pieces of evidence for some kind of long-distance relationship between a central BH and its host galaxy are the $M_{BH} - \sigma_*$ (Ferrarese and Merritt 2000; Gebhardt et al. 2000; Gültekin et al. 2009) and $M_{BH} - M_{\rm bulge}$ (Magorrian et al. 1998; Haring and Rix 2004; McConnell and Ma 2013) correlations, shown in Figs. 2.16 and 2.17, respectively. By themselves, these correlations would not necessarily imply that the AGN is having an impact on its environment. Indeed, there are many different theoretical models for the origin of these relations (e.g Somerville et al. 2001; Adams et al. 2001; Burkert and Silk 2001; King 2003; Croton et al. 2006; Kormendy and Ho 2013). However, there are many other clues that outflows and jets from AGN can affect the host galaxy evolution and morphology.

The galaxy luminosity function describes the number of galaxies as a function of luminosity and is generally modelled with the Schechter (1976) function. Theories

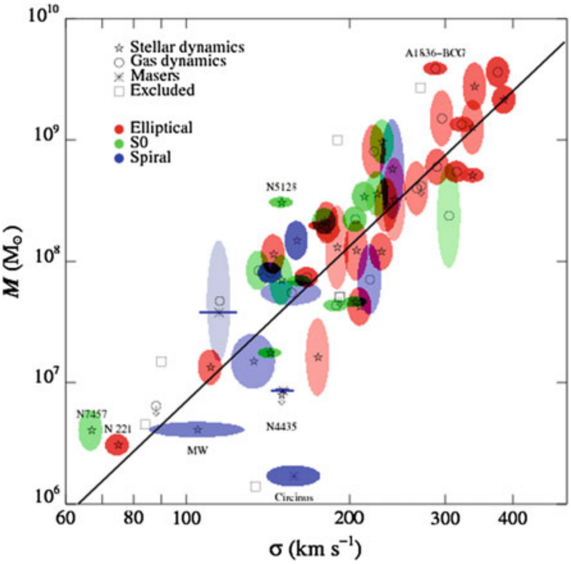

Fig. 2.16 The $M_{BH} - \sigma_*$ correlation. *Credit* Gültekin et al. (2009). Copyright AAS. Reproduced with permission

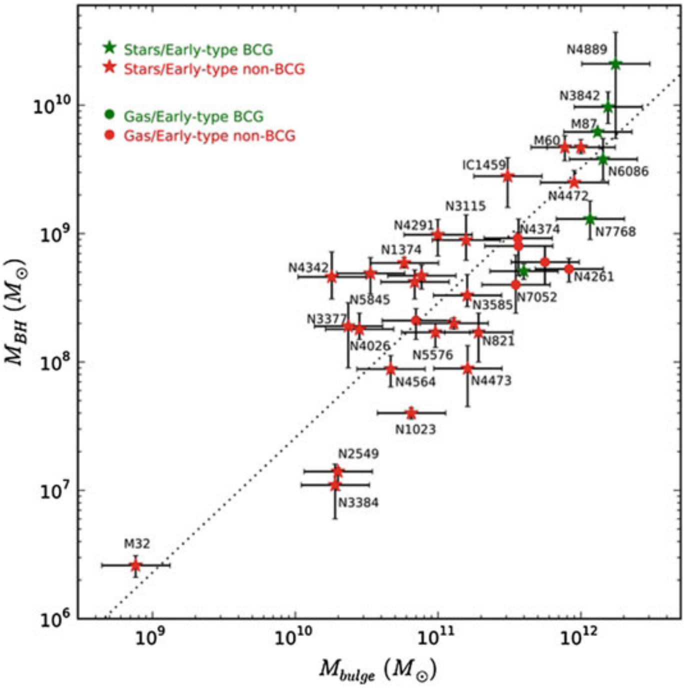

Fig. 2.17 The $M_{BH} - M_{bulge}$ correlation. *Credit* McConnell and Ma (2013). Copyright AAS. Reproduced with permission

of galaxy evolution tend to overpredict the number of galaxies at the high luminosity end, which can be avoided by invoking quenching of star formation by the central AGN (e.g. Read and Trentham 2005; Bongiorno et al. 2016). Galaxies also show bimodality in their colour distributions (Strateva et al. 2001; Bell et al. 2003; Baldry et al. 2004), with a clear separation between a blue, star-forming main sequence, and a red sequence with lower specific star formation rate (sSFR). Furthermore, these two sequences tend to lie in the same regions of colour space as the host galaxies of high and low Eddington fraction AGN, respectively, implying that the AGN may be directly responsible for quenching star formation and moving a galaxy onto the 'red and dead' branch. This has been demonstrated in several numerical simulations (e.g. Springel et al. 2005; Croton et al. 2006).

There is also evidence that AGN are energetically significant on scales larger than the galactic bulge. X-ray observations of cool core clusters and elliptical galaxies can show dramatic X-ray cavities or bubbles up to 50 kpc across, with a radio-loud AGN at the centre (Randall et al. 2011; Cavagnolo et al. 2011; Fabian 2012). This shows how radio jets can significantly impact the surrounding gas, a flavour of feedback known as 'radio' or 'kinetic' mode. These cavities also provide an estimate of the kinetic power of a radio jet, as the volume of the bubble and surrounding gas pressure gives a rough estimate of the PV work done by the jet. This can be divided by an age estimate for the cavity, giving powers of up to 10^{46} erg s^{-1}, which are weakly correlated with the radio luminosity of the source and can be large even for modest radio power (Bîrzan et al. 2008).

However, jets are not the only way for AGN to interact with their environment. I have already briefly discussed in Sect. 2.1.3.3 how fast AGN winds can drive larger-scale molecular outflows. This can be seen spectacularly in the FeLoBALQSO Mrk231, where integrated field spectroscopy shows kiloparsec-scale neutral gas outflows (Rupke and Veilleux 2011). Furthermore, King (2003) expanded on the ideas of Silk and Rees (1998) and considered a super-Eddington, momentum-driven outflow expanding into the surrounding gas. This model naturally reproduces the observed slope of the $M_{BH} - \sigma_*$ relation. This line of argument was used to suggest that super-Eddington accretion must be common near the end of a quasar cycle, although it is worth noting that line-driving, or non-radiative driving, means that super-Eddington accretion rates are not necessarily required to drive such an outflow. Intriguingly, it follows that understanding outflow physics has implications for understanding the accretion history of BHs.

2.5.2 Alternative Explanations

It cannot yet be proven that AGN are the drivers of the observed galaxy colour evolution, high-end luminosity function discrepancy or BH-bulge correlations. In particular, it is also possible that mergers are responsible for these phenomena. For example, major galaxy mergers may explain the 'red and dead' branch of the galaxy colour bimodality (e.g. Somerville et al. 2001; Baldry et al. 2004). However, AGN winds and jets are clearly energetically significant with respect to their host galaxies, so estimating their kinetic powers accurately is important in discriminating between in-situ and ex-situ scenarios.

Having established the astrophysical importance of outflows, I will now move on to discussing how we might go about accurately modelling the ionization states of accretion disc winds and their emergent spectra.

References

Abbott DC (1982) The theory of radiatively driven stellar winds. II - The line acceleration. ApJ 259:282–301. doi:10.1086/160166

Abbott DC, Lucy LB (1985) Multiline transfer and the dynamics of stellar winds. ApJ 288:679–693. doi:10.1086/162834

Adams FC, Graff DS, Richstone DO (2001) A Theoretical Model for the M_{BH}-σ Relation for Supermassive Black Holes in Galaxies. ApJ Letters 551:L31–L35. doi:10.1086/319828. arXiv:astro-ph/0010549

Allen JT, Hewett PC, Maddox N, Richards GT, Belokurov V (2011) A strong redshift dependence of the broad absorption line quasar fraction. MNRAS 410:860–884. doi:10.1111/j.1365-2966.2010.17489.x. arXiv:1007.3991

Arav N (1996) The "Ghost of LY alpha" as Evidence for Radiative Acceleration in Quasars. ApJ 465:617. doi:10.1086/177447

Arav N, Korista KT, Barlow TA, Begelman, (1995) Radiative acceleration of gas in quasars. Nature 376:576–578. doi:10.1038/376576a0

Baldry IK, Glazebrook K, Brinkmann J, Ivezić Ž, Lupton RH, Nichol RC, Szalay AS (2004) Quantifying the Bimodal Color-Magnitude Distribution of Galaxies. ApJ 600:681–694. doi:10.1086/380092. arXiv:astro-ph/0309710

Baptista R, Silveira C, Steiner JE, Horne K (2000) Spatially resolved spectra of the accretion disc of the nova-like variable UU Aquarii. MNRAS 314:713–726. doi:10.1046/j.1365-8711.2000.03325.x. arXiv:astro-ph/0002189

Barnard R, Foulkes SB, Haswell CA, Kolb U, Osborne JP, Murray JR (2006) Disc precession in the M31 dipping X-ray binary Bo 158? MNRAS 366:287–294. doi:10.1111/j.1365-2966.2005.09852.x. arXiv:astro-ph/0503259

Becker RH, White RL, Gregg MD, Brotherton MS, Laurent-Muehleisen SA, Arav N (2000) Properties of Radio-selected Broad Absorption Line Quasars from the First Bright Quasar Survey. ApJ 538:72–82. doi:10.1086/309099. arXiv:astro-ph/0002470

Begelman MC, McKee CF, Shields GA (1983) Compton heated winds and coronae above accretion disks. I Dynamics. ApJ 271:70–88. doi:10.1086/161178

Bell EF, McIntosh DH, Katz N, Weinberg MD (2003) The Optical and Near-Infrared Properties of Galaxies. I. Luminosity and Stellar Mass Functions. ApJs 149:289–312. doi:10.1086/378847. arXiv:astro-ph/0302543

Bîrzan L, McNamara BR, Nulsen PEJ, Carilli CL, Wise MW (2008) Radiative Efficiency and Content of Extragalactic Radio Sources: Toward a Universal Scaling Relation between Jet Power and Radio Power. ApJ 686:859–880. doi:10.1086/591416. arXiv:0806.1929

Blandford RD, Payne DG (1982) Hydromagnetic flows from accretion discs and the production of radio jets. MNRAS 199:883–903

Bongiorno A, Schulze A, Merloni A, Zamorani G, Ilbert O, La Franca F, Peng Y, Piconcelli E, Mainieri V, Silverman JD, Brusa M, Fiore F, Salvato M, Scoville N (2016) GN host galaxy mass function in COSMOS. Is AGN feedback responsible for the mass-quenching of galaxies? AAP 588:A78. doi:10.1051/0004-6361/201527436, 1601.02091

Borguet BCJ, Edmonds D, Arav N, Dunn J, Kriss GA (2012) A 10 kpc Scale Seyfert Galaxy Outflow: HST/COS Observations of IRAS F22456–5125. ApJ 751:107. doi:10.1088/0004-637X/751/2/107. arXiv:1205.0189

Borguet BCJ, Arav N, Edmonds D, Chamberlain C, Benn C (2013) Major Contributor to AGN Feedback: VLT X-shooter Observations of S IV BALQSO Outflows. ApJ 762:49. doi:10.1088/0004-637X/762/1/49. arXiv:1211.6250

Borguet B, Hutsemékers D (2010) polar+equatorial wind model for broad absorption line quasars. I. Fitting the C IV BAL profiles. AAP 515:A22. doi:10.1051/0004-6361/200913255. 1003.2386

Boroson TA, Meyers KA (1992) The optical properties of IR-selected and MG II broad absorption line quasars. ApJ 397:442–451. doi:10.1086/171800

Bowler RAA, Hewett PC, Allen JT, Ferland GJ (2014) Line-driven radiative outflows in luminous quasars. MNRAS 445:359–377. doi:10.1093/mnras/stu1730. arXiv:1408.5808

Braito V, Reeves JN, Dewangan GC, George I, Griffiths RE, Markowitz A, Nandra K, Porquet D, Ptak A, Turner TJ, Yaqoob T, Weaver K (2007) Relativistic Iron K Emission and Absorption in the Seyfert 1.9 Galaxy MCG -5-23-16. ApJ 670:978–991. doi:10.1086/521916. arXiv:0707.2950

Brown JC, Richardson LL, Antokhin I, Robert C, Moffat AFJ, St-Louis N (1995) Combined spectrometric, photometric and polarimetric diagnostics for 'blobs' in WR star winds. A&A 295:725

Burkert A, Silk J (2001) Star Formation-Regulated Growth of Black Holes in Protogalactic Spheroids. ApJ Letters 554:L151–L154. doi:10.1086/321698. arXiv:astro-ph/0011511

Capellupo DM, Hamann F, Shields JC, Rodríguez Hidalgo P, Barlow TA (2011) Variability in quasar broad absorption line outflows - I. Trends in the short-term versus long-term data. MNRAS 413:908–920. doi:10.1111/j.1365-2966.2010.18185.x. arXiv:1012.2336

Capellupo DM, Hamann F, Shields JC, Rodríguez Hidalgo P, Barlow TA (2012) Variability in quasar broad absorption line outflows - II. Multi-epoch monitoring of Si IV and C IV broad absorption line variability. MNRAS 422:3249–3267. doi:10.1111/j.1365-2966.2012.20846.x. arXiv:1203.1051

Capellupo DM, Hamann F, Barlow TA (2014) A variable P v broad absorption line and quasar outflow energetics. MNRAS 444:1893–1900. doi:10.1093/mnras/stu1502. arXiv:1407.7532

Cappi M, Mihara T, Matsuoka M, Hayashida K, Weaver KA, Otani C (1996) Warm Absorber, Reflection, and Fe K Line in the X-Ray Spectrum of IC 4329A. ApJ 458:149. doi:10.1086/176799. arXiv:astro-ph/9510065

Castor JL (1974) On the force associated with absorption of spectral line radiation. MNRAS 169:279–306

Castor JI, Abbott DC, Klein RI (1975) Radiation-driven winds in Of stars. ApJ 195:157–174. doi:10.1086/153315

Cavagnolo KW, McNamara BR, Wise MW, Nulsen PEJ, Brüggen M, Gitti M, Rafferty DA (2011) A Powerful AGN Outburst in RBS 797. ApJ 732:71. doi:10.1088/0004-637X/732/2/71. arXiv:1103.0630

Chamberlain C, Arav N, Benn C (2015) Strong candidate for AGN feedback: VLT/X-shooter observations of BALQSO SDSS J0831+0354. MNRAS 450:1085–1093. doi:10.1093/mnras/stv572

Chen B, Dai X, Baron E (2013a) Inclination-dependent Active Galactic Nucleus Flux Profiles from Strong Lensing of the Kerr Spacetime. ApJ 762:122. doi:10.1088/0004-637X/762/2/122. arXiv:1211.2510

Chen B, Dai X, Baron E, Kantowski R (2013b) Effects of Kerr Strong Gravity on Quasar X-Ray Microlensing. ApJ 769:131. doi:10.1088/0004-637X/769/2/131. arXiv:1211.6487

Church MJ, Reed D, Dotani T, Bałucińska-Church M, Smale AP (2005) Discovery of absorption features of the accretion disc corona and systematic acceleration of the X-ray burst rate in XB1323-619. MNRAS 359:1336–1344. doi:10.1111/j.1365-2966.2005.08728.x. arXiv:astro-ph/0412228

Clavel J, Schartel N, Tomas L (2006) Long observations of the BALQSO LBQS 2212–1759 with XMM-Newton. A&A 446:439–446. doi:10.1051/0004-6361:20041963. arXiv:astro-ph/0509432

Cohen MH, Ogle PM, Tran HD, Vermeulen RC, Miller JS, Goodrich RW, Martel AR (1995) Spectropolarimetry of Two Broad Absorption Line Quasars with the W. M. Keck Telescope. ApJ Letters 448:L77. doi:10.1086/309602

Connolly SD, McHardy IM, Dwelly T (2014) Long-term wind-driven X-ray spectral variability of NGC 1365 with Swift. MNRAS 440:3503–3510. doi:10.1093/mnras/stu546. arXiv:1403.4253

Cordova FA, Mason KO (1982) High-velocity winds from a dwarf nova during outburst. ApJ 260:716–721. doi:10.1086/160291

Cottis CE, Goad MR, Knigge C, Scaringi S (2010) Searching for the signature of radiative line driving: on the absence of Lyα-NV line-locking features in a large sample of BALQSOs. MNRAS 406:2094–2112. doi:10.1111/j.1365-2966.2010.16839.x. arXiv:1004.2145

Crenshaw DM, Kraemer SB (2012) Feedback from Mass Outflows in Nearby Active Galactic Nuclei. I. Ultraviolet and X-Ray Absorbers. ApJ 753:75. doi:10.1088/0004-637X/753/1/75. arXiv:1204.6694

Crenshaw DM, Kraemer SB, Gabel JR, Kaastra JS, Steenbrugge KC, Brinkman AC, Dunn JP, George IM, Liedahl DA, Paerels FBS, Turner TJ, Yaqoob T (2003) Simultaneous Ultraviolet and X-Ray Spectroscopy of the Seyfert 1 Galaxy NGC 5548. I. Physical Conditions in the Ultraviolet Absorbers. ApJ 594:116–127. doi:10.1086/376792. arXiv:astro-ph/0305154

Croton DJ, Springel V, White SDM, De Lucia G, Frenk CS, Gao L, Jenkins A, Kauffmann G, Navarro JF, Yoshida N (2006) The many lives of active galactic nuclei: cooling flows, black holes and the luminosities and colours of galaxies. MNRAS 365:11–28. doi:10.1111/j.1365-2966.2005.09675.x. arXiv:astro-ph/0508046

Dai X, Shankar F, Sivakoff GR (2008) 2MASS Reveals a Large Intrinsic Fraction of BALQSOs. ApJ 672:108–114. doi:10.1086/523688. arXiv:0704.2882
Dai X, Shankar F, Sivakoff GR (2012) The Intrinsic Fractions and Radio Properties of Low-ionization Broad Absorption Line Quasars. ApJ 757:180. doi:10.1088/0004-637X/757/2/180. arXiv:1004.0700
de Kool M, Begelman MC (1995) Radiation Pressure-driven Magnetic Disk Winds in Broad Absorption Line Quasi-stellar Objects. ApJ 455:448. doi:10.1086/176594
Done C, Jin C (2015) The Mass and Spin of The Extreme Narrow Line Seyfert 1 Galaxy 1H0707-495 and Its Implications for The Trigger for Relativistic Jets. ArXiv e-prints arXiv:1506.04547
Drew J, Verbunt F (1985) Investigation of a wind model for cataclysmic variable ultraviolet resonance line emission. MNRAS 213:191–213
Elvis M (2000) A Structure for Quasars. ApJ 545:63–76. DOI 10.1086/317778, arXiv:arXiv:astro-ph/0008064
Fabian AC (2012) Observational Evidence of Active Galactic Nuclei Feedback. ARAA 50:455–489. doi:10.1146/annurev-astro-081811-125521. arXiv:1204.4114
Fabian AC, Kunieda H, Inoue S, Matsuoka M, Mihara T, Miyamoto S, Otani C, Ricker G, Tanaka Y, Yamauchi M, Yaqoob T (1994) ASCA observations of the warm absorber in MCG-6-30-15: The discovery of a change in column density. PASJ 46:L59–L63
Feldmeier A (1995) Time-dependent structure and energy transfer in hot star winds. A&A 299:523
Ferrarese L, Merritt D (2000) A Fundamental Relation between Supermassive Black Holes and Their Host Galaxies. ApJ Letters 539:L9–L12. doi:10.1086/312838. arXiv:astro-ph/0006053
Filiz Ak N, Brandt WN, Hall PB, Schneider DP, Anderson SF, Gibson RR, Lundgren BF, Myers AD, Petitjean P, Ross NP, Shen Y, York DG, Bizyaev D, Brinkmann J, Malanushenko E, Oravetz DJ, Pan K, Simmons AE, Weaver BA (2012) Broad Absorption Line Disappearance on Multi-year Timescales in a Large Quasar Sample. ApJ 757:114. doi:10.1088/0004-637X/757/2/114. arXiv:1208.0836
Flohic HMLG, Eracleous M, Bogdanović T (2012) Effects of an Accretion Disk Wind on the Profile of the Balmer Emission Lines from Active Galactic Nuclei. ApJ 753:133. doi:10.1088/0004-637X/753/2/133
Foltz CB, Weymann RJ, Morris SL, Turnshek DA (1987) The complex absorption spectrum of the broad absorption line QSO 1303 + 308. ApJ 317:450–459. doi:10.1086/165290
Friend DB, Abbott DC (1986) The theory of radiatively driven stellar winds. III - Wind models with finite disk correction and rotation. ApJ 311:701–707. doi:10.1086/164809
Fukumura K, Tombesi F, Kazanas D, Shrader C, Behar E, Contopoulos I (2015) Magnetically Driven Accretion Disk Winds and Ultra-fast Outflows in PG 1211+143. ApJ 805:17. doi:10.1088/0004-637X/805/1/17. arXiv:1503.04074
Gallagher SC, Brandt WN, Sambruna RM, Mathur S, Yamasaki N (1999) Exploratory ASCA Observations of Broad Absorption Line Quasi-stellar Objects. ApJ 519:549–555. doi:10.1086/307405. arXiv:astro-ph/9902045
Gallagher SC, Brandt WN, Chartas G, Garmire GP (2002) X-Ray Spectroscopy of Quasi-Stellar Objects with Broad Ultraviolet Absorption Lines. ApJ 567:37–41. doi:10.1086/338485. arXiv:astro-ph/0110579
Ganguly R, Bond NA, Charlton JC, Eracleous M, Brandt WN, Churchill CW (2001) On the Origin of Intrinsic Narrow Absorption Lines in $z \lesssim 1$ QSOS. ApJ 549:133–154. doi:10.1086/319082. arXiv:astro-ph/0010192
Ganguly R, Sembach KR, Tripp TM, Savage BD, Wakker BP (2006) High-Resolution Absorption Spectroscopy of Multiphase, High-Metallicity Gas Associated with the Luminous Quasar HE 0226–4110. ApJ 645:868–889. doi:10.1086/504395. arXiv:astro-ph/0603492
Gebhardt K, Bender R, Bower G, Dressler A, Faber SM, Filippenko AV, Green R, Grillmair C, Ho LC, Kormendy J, Lauer TR, Magorrian J, Pinkney J, Richstone D, Tremaine S (2000) A Relationship between Nuclear Black Hole Mass and Galaxy Velocity Dispersion. ApJ Letters 539:L13–L16. doi:10.1086/312840. arXiv:astro-ph/0006289

Ghosh KK, Punsly B (2007) The Physical Nature of Polar Broad Absorption Line Quasars. ApJ Letters 661:L139–L142. doi:10.1086/518859. arXiv:0704.2407

Gibson RR, Jiang L, Brandt WN, Hall PB, Shen Y, Wu J, Anderson SF, Schneider DP, Vanden Berk D, Gallagher SC, Fan X, York DG (2009) A Catalog of Broad Absorption Line Quasars in Sloan Digital Sky Survey Data Release 5. ApJ 692:758–777. doi:10.1088/0004-637X/692/1/758. arXiv:0810.2747

Giustini M, Cappi M, Chartas G, Dadina M, Eracleous M, Ponti G, Proga D, Tombesi F, Vignali C, Palumbo GGC (2011) Variable X-ray absorption in the mini-BAL QSO PG 1126–041. A&A 536:A49. doi:10.1051/0004-6361/201117732. arXiv:1109.6026

Gofford J, Reeves JN, Tombesi F, Braito V, Turner TJ, Miller L, Cappi M (2013) The Suzaku view of highly ionized outflows in AGN - I. Statistical detection and global absorber properties. MNRAS 430:60–80. doi:10.1093/mnras/sts481. arXiv:1211.5810

Gofford J, Reeves JN, Braito V, Nardini E, Costa MT, Matzeu GA, O'Brien P, Ward M, Turner TJ, Miller L (2014) Revealing the Location and Structure of the Accretion Disk Wind in PDS 456. ApJ 784:77. doi:10.1088/0004-637X/784/1/77. arXiv:1402.3700

Gofford J, Reeves JN, McLaughlin DE, Braito V, Turner TJ, Tombesi F, Cappi M (2015) The Suzaku view of highly ionized outflows in AGN - II. Location, energetics and scalings with bolometric luminosity. MNRAS 451:4169–4182. doi:10.1093/mnras/stv1207. arXiv:1506.00614

Goodrich RW (1997) On the Fraction of Broad Absorption Line Quasi-stellar Objects. ApJ 474:606–611

Goodrich RW, Miller JS (1995) Polarization Clues to the Structure of Broad Absorption Line Quasi-stellar Objects. ApJ Letters 448:L73. doi:10.1086/309600

Green PJ, Aldcroft TL, Mathur S, Wilkes BJ, Elvis M (2001) A Chandra Survey of Broad Absorption Line Quasars. ApJ 558:109–118. doi:10.1086/322311. arXiv:astro-ph/0105258

Greenstein JL, Oke JB (1982) RW Sextantis, a disk with a hot, high-velocity wind. ApJ 258:209–216. doi:10.1086/160069

Groot PJ, Rutten RGM, van Paradijs J (2004) A spectrophotometric study of RW Trianguli. A&A 417:283–291. doi:10.1051/0004-6361:20031771. arXiv:astro-ph/0401029

Grupe D, Mathur S, Elvis M (2003a) XMM-Newton Observations of Two Broad Absorption Line QSOs: Q1246-057 and SBS 1542+541. AJ 126:1159–1166. doi:10.1086/377141. arXiv:astro-ph/0305309

Grupe D, Nousek JA (2015) Is There a Connection between Broad Absorption Line Quasars and Narrow-Line Seyfert 1 Galaxies? AJ 149:85. doi:10.1088/0004-6256/149/2/85. arXiv:1412.8256

Gültekin K, Richstone DO, Gebhardt K, Lauer TR, Tremaine S, Aller MC, Bender R, Dressler A, Faber SM, Filippenko AV, Green R, Ho LC, Kormendy J, Magorrian J, Pinkney J, Siopis C (2009) The M-σ and M-L Relations in Galactic Bulges, and Determinations of Their Intrinsic Scatter. ApJ 698:198–221. doi:10.1088/0004-637X/698/1/198. arXiv:0903.4897

Hall PB, Anderson SF, Strauss MA, York DG, Richards GT, Fan X, Knapp GR, Schneider DP, Vanden Berk DE, Geballe TR, Bauer AE, Becker RH, Davis M, Rix HW, Nichol RC, Bahcall NA, Brinkmann J, Brunner R, Connolly AJ, Csabai I, Doi M, Fukugita M, Gunn JE, Haiman Z, Harvanek M, Heckman TM, Hennessy GS, Inada N, Ivezić Ž, Johnston D, Kleinman S, Krolik JH, Krzesinski J, Kunszt PZ, Lamb DQ, Long DC, Lupton RH, Miknaitis G, Munn JA, Narayanan VK, Neilsen E, Newman PR, Nitta A, Okamura S, Pentericci L, Pier JR, Schlegel DJ, Snedden S, Szalay AS, Thakar AR, Tsvetanov Z, White RL, Zheng W (2002) Unusual Broad Absorption Line Quasars from the Sloan Digital Sky Survey. ApJs 141:267–309. doi:10.1086/340546. arXiv:astro-ph/0203252

Hall PB, Anosov K, White RL, Brandt WN, Gregg MD, Gibson RR, Becker RH, Schneider DP (2011) Implications of dramatic broad absorption line variability in the quasar FBQS J1408+3054. MNRAS 411:2653–2666. doi:10.1111/j.1365-2966.2010.17870.x. arXiv:1010.3728

Halpern JP (1984) Variable X-ray absorption in the QSO MR 2251–178. ApJ 281:90–94. doi:10.1086/162077

Hamann WR, Oskinova LM, Feldmeier A (2008) Spectrum formation in clumpy stellar winds. In: Hamann WR, Feldmeier A, Oskinova LM (eds) Clumping in Hot-Star Winds, p 75

Hamann WR, Leuenhagen U, Koesterke L, Wessolowski U (1992) Modelling the spectrum of WC-type Wolf-Rayet stars. A&A 255:200–214

Hamann WR, Wessolowski U, Koesterke L (1994) Non-LTE spectral analyses of Wolf-Rayet stars: The nitrogen spectrum of the WN6 prototype HD 192163 (WR136). A&A 281:184–198

Hamann F, Chartas G, McGraw S, Rodriguez Hidalgo P, Shields J, Capellupo D, Charlton J, Eracleous M (2013) Extreme-velocity quasar outflows and the role of X-ray shielding. MNRAS 435:133–148. doi:10.1093/mnras/stt1231. arXiv:1307.1173

Häring N, Rix HW (2004) On the Black Hole Mass-Bulge Mass Relation. ApJ Letters 604:L89–L92. doi:10.1086/383567. arXiv:arXiv:astro-ph/0402376

Hazard C, Morton DC, Terlevich R, McMahon R (1984) Nine new quasi-stellar objects with broad absorption lines. ApJ 282:33–52. doi:10.1086/162174

Heap SR, Boggess A, Holm A, Klinglesmith DA, Sparks W, West D, Wu CC, Boksenberg A, Willis A, Wilson R, Macchetto F, Selvelli PO, Stickland D, Greenstein JL, Hutchings JB, Underhill AB, Viotti R, Whelan JAJ (1978) IUE observations of hot stars - HZ43, BD +75 deg 325, NGC 6826, SS Cygni, Eta Carinae. Nature 275:385–388. doi:10.1038/275385a0

Higginbottom N, Knigge C, Long KS, Sim SA, Matthews JH (2013) A simple disc wind model for broad absorption line quasars. MNRAS 436:1390–1407. doi:10.1093/mnras/stt1658. arXiv:1308.5973

Higginbottom N, Proga D, Knigge C, Long KS, Matthews JH, Sim SA (2014) Line-driven Disk Winds in Active Galactic Nuclei: The Critical Importance of Ionization and Radiative Transfer. ApJ 789:19. doi:10.1088/0004-637X/789/1/19. arXiv:1402.1849

Hillier DJ (1984) The influence of electron scattering on the He II line profiles in HD 50896. ApJ 280:744–748. doi:10.1086/162047

Hillier DJ (1991) The effects of electron scattering and wind clumping for early emission line stars. A&A 247:455–468

Ioannou Z, van Zyl L, Naylor T, Charles PA, Margon B, Koch-Miramond L, Ilovaisky S (2003) Understanding the LMXB X2127+119 in M 15. II. The UV data. A&A 399:211–218. doi:10.1051/0004-6361:20021578. arXiv:astro-ph/0212127

Kaastra JS, Mewe R, Liedahl DA, Komossa S, Brinkman AC (2000) X-ray absorption lines in the Seyfert 1 galaxy NGC 5548 discovered with Chandra-LETGS. A&A 354:L83–L86 arXiv:astro-ph/0002345

Kaastra JS, Kriss GA, Cappi M, Mehdipour M, Petrucci PO, Steenbrugge KC, Arav N, Behar E, Bianchi S, Boissay R, Branduardi-Raymont G, Chamberlain C, Costantini E, Ely JC, Ebrero J, Di Gesu L, Harrison FA, Kaspi S, Malzac J, De Marco B, Matt G, Nandra K, Paltani S, Person R, Peterson BM, Pinto C, Ponti G, Nuñez FP, De Rosa A, Seta H, Ursini F, de Vries CP, Walton DJ, Whewell M (2014) A fast and long-lived outflow from the supermassive black hole in NGC 5548. Science 345:64–68. doi:10.1126/science.1253787. arXiv:1406.5007

Kafka S, Honeycutt RK (2004) Detecting Outflows from Cataclysmic Variables in the Optical. AJ 128:2420–2429. doi:10.1086/424618

King A (2003) Black Holes, Galaxy Formation, and the M_{BH}-σ Relation. ApJ Letters 596:L27–L29. doi:10.1086/379143. arXiv:astro-ph/0308342

Knigge C, Drew JE (1997) Eclipse Mapping of the Accretion Disk Wind in the Cataclysmic Variable UX Ursae Majoris. ApJ 486:445–456

Knigge C, Woods JA, Drew JE (1995) The application of Monte Carlo methods to the synthesis of spectral line profiles arising from accretion disc winds. MNRAS 273:225–248

Knigge C, Long KS, Blair WP, Wade RA (1997) Disks, Winds, and Veiling Curtains: Dissecting the Ultraviolet Spectrum of the Dwarf Nova Z Camelopardalis in Outburst. ApJ 476:291–310

Knigge C, Scaringi S, Goad MR, Cottis CE (2008) The intrinsic fraction of broad-absorption line quasars. MNRAS 386:1426–1435. doi:10.1111/j.1365-2966.2008.13081.x. arXiv:0802.3697

Konigl A, Kartje JF (1994) Disk-driven hydromagnetic winds as a key ingredient of active galactic nuclei unification schemes. ApJ 434:446–467. doi:10.1086/174746

Kormendy J, Ho LC (2013) Coevolution (Or Not) of Supermassive Black Holes and Host Galaxies. ARAA 51:511–653. doi:10.1146/annurev-astro-082708-101811. arXiv:1304.7762

Kotani T, Ebisawa K, Dotani T, Inoue H, Nagase F, Tanaka Y, Ueda Y (2000) ASCA Observations of the Absorption Line Features from the Superluminal Jet Source GRS 1915+105. ApJ 539:413–423. doi:10.1086/309200. arXiv:astro-ph/0003237

Kriss GA, Krolik JH, Otani C, Espey BR, Turner TJ, Kii T, Tsvetanov Z, Takahashi T, Davidsen AF, Tashiro M, Zheng W, Murakami S, Petre R, Mihara T (1996) ASCA Observations of the Composite Warm Absorber in NGC 3516. ApJ 467:629. doi:10.1086/177638. arXiv:astro-ph/9603057

Krolik JH, Kriss GA (2001) Warm Absorbers in Active Galactic Nuclei: A Multitemperature Wind. ApJ 561:684–690. doi:10.1086/323442

Krolik JH, Voit GM (1998) What Is the True Covering Factor of Absorbing Matter in BALQSOs? ApJ Letters 497:L5–L8. doi:10.1086/311274. arXiv:astro-ph/9802082

Kudoh T, Shibata K (1997) Magnetically Driven Jets from Accretion Disks. I. Steady Solutions and Application to Jets/Winds in Young Stellar Objects. ApJ 474:362–377

Kusterer DJ, Nagel T, Hartmann S, Werner K, Feldmeier A (2014) Monte Carlo radiation transfer in CV disk winds: application to the AM CVn prototype. A&A 561:A14. doi:10.1051/0004-6361/201321438

Long KS, Knigge C (2002) Modeling the Spectral Signatures of Accretion Disk Winds: A New Monte Carlo Approach. APJ 579:725–740. doi:10.1086/342879. arXiv:astro-ph/0208011

Lucy LB, Solomon PM (1970) Mass Loss by Hot Stars. ApJ 159:879. doi:10.1086/150365

MacGregor KB, Hartmann L, Raymond JC (1979) Radiative amplification of sound waves in the winds of O and B stars. ApJ 231:514–523. doi:10.1086/157213

Magorrian J, Tremaine S, Richstone D, Bender R, Bower G, Dressler A, Faber SM, Gebhardt K, Green R, Grillmair C, Kormendy J, Lauer T (1998) The Demography of Massive Dark Objects in Galaxy Centers. AJ 115:2285–2305. doi:10.1086/300353. arXiv:astro-ph/9708072

Matthews JH, Knigge C, Long KS, Sim SA, Higginbottom N, Mangham SW (2016) Testing quasar unification: radiative transfer in clumpy winds. MNRAS 458:293–305. doi:10.1093/mnras/stw323. arXiv:1602.02765

Matthews JH, Knigge C, Long KS, Sim SA, Higginbottom N (2015) The impact of accretion disc winds on the optical spectra of cataclysmic variables. MNRAS 450:3331–3344. doi:10.1093/mnras/stv867

Matzeu GA, Reeves JN, Nardini E, Braito V, Costa MT, Tombesi F, Gofford J (2016) Short-term X-ray spectral variability of the quasar PDS 456 observed in a low-flux state. MNRAS 458:1311–1329. doi:10.1093/mnras/stw354. arXiv:1602.04023

Mauche CW, Raymond JC (1987) IUE observations of the dwarf nova HL Canis Majoris and the winds of cataclysmic variables. ApJ 323:690–713. doi:10.1086/165865

McConnell NJ, Ma CP (2013) Revisiting the Scaling Relations of Black Hole Masses and Host Galaxy Properties. ApJ 764:184. doi:10.1088/0004-637X/764/2/184. arXiv:1211.2816

Misawa T, Charlton JC, Eracleous M, Ganguly R, Tytler D, Kirkman D, Suzuki N, Lubin D (2007) A Census of Intrinsic Narrow Absorption Lines in the Spectra of Quasars at z = 2–4. ApJs 171:1–28. doi:10.1086/513713. arXiv:astro-ph/0702101

Misawa T, Eracleous M, Chartas G, Charlton JC (2008) Exploratory Study of the X-Ray Properties of Quasars with Intrinsic Narrow Absorption Lines. ApJ 677:863–879. doi:10.1086/529426. arXiv:0801.1692

Morabito LK, Dai X, Leighly KM, Sivakoff GR, Shankar F (2013) Unveiling the Intrinsic X-ray Properties of Broad Absorption Line Quasars with a Relatively Unbiased Sample. ArXiv e-prints arXiv:1309.5978

Murray N, Chiang J (1996) Wind-dominated optical line emission from accretion disks around luminous cataclysmic variable stars. Nature 382:789–791. doi:10.1038/382789a0

Murray N, Chiang J (1997) Disk Winds and Disk Emission Lines. ApJ 474:91–103

Murray N, Chiang J, Grossman SA, Voit GM (1995) Accretion Disk Winds from Active Galactic Nuclei. ApJ 451:498. doi:10.1086/176238

Nardini E, Reeves JN, Gofford J, Harrison FA, Risaliti G, Braito V, Costa MT, Matzeu GA, Walton DJ, Behar E, Boggs SE, Christensen FE, Craig WW, Hailey CJ, Matt G, Miller JM, O'Brien

PT, Stern D, Turner TJ, Ward MJ (2015) Black hole feedback in the luminous quasar PDS 456. Science 347:860–863. doi:10.1126/science.1259202. arXiv:1502.06636

Nestor D, Hamann F, Rodriguez Hidalgo P (2008) The quasar-frame velocity distribution of narrow CIV absorbers. MNRAS 386:2055–2064. doi:10.1111/j.1365-2966.2008.13156.x. arXiv:0803.0326

Noebauer UM, Long KS, Sim SA, Knigge C (2010) The Geometry and Ionization Structure of the Wind in the Eclipsing Nova-like Variables RW Tri and UX UMa. ApJ 719:1932–1945. doi:10.1088/0004-637X/719/2/1932. arXiv:1007.0209

North M, Knigge C, Goad M (2006) A new sample of broad absorption-line quasars exhibiting the ghost of Lyman α. MNRAS 365:1057–1066. doi:10.1111/j.1365-2966.2005.09828.x. arXiv:astro-ph/0511133

O'Dowd MJ, Bate NF, Webster RL, Labrie K, Rogers J (2015) Microlensing Constraints on Broad Absorption and Emission Line Flows in the Quasar H1413+117. ArXiv e-prints arXiv:1504.07160

Orr A, Molendi S, Fiore F, Grandi P, Parmar AN, Owens A (1997) Soft X-ray observations of the complex warm absorber in MCG-6-30-15 with BeppoSAX. A&A 324:L77–L80 arXiv:astro-ph/9706133

Otani C, Kii T, Reynolds CS, Fabian AC, Iwasawa K, Hayashida K, Inoue H, Kunieda H, Makino F, Matsuoka M, Tanaka Y (1996) The Variable O, VIII Warm Absorber in MCG-6-30-15. PASJ 48:211–218. doi:10.1093/pasj/48.2.211. arXiv:astro-ph/9511063

Ouyed R, Pudritz RE (1997) Numerical Simulations of Astrophysical Jets from Keplerian Disks. I. Stationary Models. ApJ 482:712–732

Owocki S (2014) Theory of Winds from Hot. Luminous Massive Stars, ArXiv e-prints arXiv:1409.2084

Owocki SP, Rybicki GB (1984) Instabilities in line-driven stellar winds. I - Dependence on perturbation wavelength. ApJ 284:337–350. doi:10.1086/162412

Owocki SP, Rybicki GB (1985) Instabilities in line-driven stellar winds. II - Effect of scattering. ApJ 299:265–276. doi:10.1086/163697

Owocki SP, Castor JI, Rybicki GB (1988) Time-dependent models of radiatively driven stellar winds. I - Nonlinear evolution of instabilities for a pure absorption model. ApJ 335:914–930. doi:10.1086/166977

Parmar AN, Oosterbroek T, Boirin L, Lumb D (2002) Discovery of narrow X-ray absorption features from the dipping low-mass X-ray binary X 1624–490 with XMM-Newton. A&A 386:910–915. doi:10.1051/0004-6361:20020281. arXiv:astro-ph/0202452

Patterson J, Patino R, Thorstensen JR, Harvey D, Skillman DR, Ringwald FA (1996) Periods and Quasiperiods in the Cataclysmic Variable BZ Camelopardalis. AJ 111:2422. doi:10.1086/117976

Pauldrach A, Puls J, Kudritzki RP (1986) Radiation-driven winds of hot luminous stars - Improvements of the theory and first results. A&A 164:86–100

Pauldrach AWA, Kudritzki RP, Puls J, Butler K, Hunsinger J (1994) Radiation-driven winds of hot luminous stars. 12: A first step towards detailed UV-line diagnostics of O-stars. A&A 283:525–560

Pelletier G, Pudritz RE (1992) Hydromagnetic disk winds in young stellar objects and active galactic nuclei. ApJ 394:117–138. doi:10.1086/171565

Pereyra NA, Kallman TR, Blondin JM (1997) Hydrodynamical Models of Line-driven Accretion Disk Winds. ApJ 477:368–378

Ponti G, Fender RP, Begelman MC, Dunn RJH, Neilsen J, Coriat M (2012) Ubiquitous equatorial accretion disc winds in black hole soft states. MNRAS 422:L11. doi:10.1111/j.1745-3933.2012.01224.x. arXiv:1201.4172

Pounds KA, Reeves JN (2009) Quantifying the fast outflow in the luminous Seyfert galaxy PG1211+143. MNRAS 397:249–257. doi:10.1111/j.1365-2966.2009.14971.x. arXiv:0811.3108

Pounds K, Lobban A, Reeves J, Vaughan S (2016) Detection of a second high-velocity component in the highly ionized wind from PG 1211+143. MNRAS 457:2951–2957. doi:10.1093/mnras/stw165. arXiv:1601.05367

Prinja RK, Smith LJ (1992) Migrating optical depth enhancements in the UV wind lines of the Wolf-Rayet star HD 93131. A&A 266:377–384

Proga D (2005) Theory of Outflows in Cataclysmic Variables. In: Hameury JM, Lasota JP (eds) The Astrophysics of Cataclysmic Variables and Related Objects, Astronomical Society of the Pacific Conference Series, vol 330, p 103, arXiv:astro-ph/0411200

Proga D (2003) Numerical Simulations of Mass Outflows Driven from Accretion Disks by Radiation and Magnetic Forces. ApJ 585:406–417. doi:10.1086/345897. arXiv:astro-ph/0210642

Proga D, Stone JM, Drew JE (1998) Radiation-driven winds from luminous accretion discs. MNRAS 295:595. doi:10.1046/j.1365-8711.1998.01337.x. arXiv:astro-ph/9710305

Proga D, Kallman TR, Drew JE, Hartley LE (2002a) Resonance Line Profile Calculations Based on Hydrodynamical Models of Cataclysmic Variable Winds. ApJ 572:382–391. doi:10.1086/340339. arXiv:astro-ph/0202384

Proga D, Kallman TR (2004) Dynamics of Line-driven Disk Winds in Active Galactic Nuclei. II. Effects of Disk Radiation. ApJ 616:688–695. doi:10.1086/425117. arXiv:arXiv:astro-ph/0408293

Proga D, Stone JM, Kallman TR (2000) Dynamics of Line-driven Disk Winds in Active Galactic Nuclei. ApJ 543:686–696. doi:10.1086/317154. arXiv:arXiv:astro-ph/0005315

Puebla RE, Diaz MP, Hillier DJ, Hubeny I (2011) A Method for the Study of Accretion Disk Emission in Cataclysmic Variables. I. The Model. ApJ 736:17. doi:10.1088/0004-637X/736/1/17. arXiv:1105.0851

Randall SW, Forman WR, Giacintucci S, Nulsen PEJ, Sun M, Jones C, Churazov E, David LP, Kraft R, Donahue M, Blanton EL, Simionescu A, Werner N (2011) Shocks and Cavities from Multiple Outbursts in the Galaxy Group NGC 5813: A Window to Active Galactic Nucleus Feedback. ApJ 726:86. doi:10.1088/0004-637X/726/2/86. arXiv:1006.4379

Read JI, Trentham N (2005) The baryonic mass function of galaxies. Philosophical Transactions of the Royal Society of London Series A 363. doi:10.1098/rsta.2005.1648. arXiv:astro-ph/0502517

Reeves JN, Wynn G, O'Brien PT, Pounds KA (2002) Extreme X-ray variability in the luminous quasar PDS 456. MNRAS 336:L56–L60. doi:10.1046/j.1365-8711.2002.06038.x. arXiv:astro-ph/0209120

Reeves JN, O'Brien PT, Ward MJ (2003) A Massive X-Ray Outflow from the Quasar PDS 456. ApJ Letters 593:L65–L68. doi:10.1086/378218. arXiv:astro-ph/0307127

Reichard TA, Richards GT, Hall PB, Schneider DP, Vanden Berk DE, Fan X, York DG, Knapp GR, Brinkmann J (2003) Continuum and Emission-Line Properties of Broad Absorption Line Quasars. AJ 126:2594–2607. doi:10.1086/379293. arXiv:arXiv:astro-ph/0308508

Reynolds CS, Fabian AC (1995) Warm absorbers in active galactic nuclei. MNRAS 273:1167–1176. doi:10.1093/mnras/273.4.1167. arXiv:astro-ph/9502006

Ringwald FA, Naylor T (1998) High-speed optical spectroscopy of a cataclysmic variable wind–BZ Camelopardalis. AJ 115:286. doi:10.1086/300192. astro-ph/9710021

Romanova MM, Ustyugova GV, Koldoba AV, Chechetkin VM, Lovelace RVE (1997) Formation of Stationary Magnetohydrodynamic Outflows from a Disk by Time-dependent Simulations. ApJ 482:708–711

Rupke DSN, Veilleux S (2011) Integral Field Spectroscopy of Massive, Kiloparsec-scale Outflows in the Infrared-luminous QSO Mrk 231. ApJ Letters 729:L27. doi:10.1088/2041-8205/729/2/L27. arXiv:1102.4349

Sabra BM, Hamann F (2001) PG 1254+047: An Intrinsically X-Ray Weak, Heavily Absorbed Broad Absorption Line Quasar? ApJ 563:555–559. doi:10.1086/324043

Schechter P (1976) An analytic expression for the luminosity function for galaxies. ApJ 203:297–306. doi:10.1086/154079

Schmutz W (1997) Photon loss from the helium Lyα line - the key to the acceleration of Wolf-Rayet winds. A&A 321:268–287

Shaw AW, Gandhi P, Altamirano D, Uttley P, Tomsick JA, Charles PA, Fürst F, Rahoui F, Walton DJ (2016) A low-luminosity soft state in the short-period black hole X-ray binary Swift J1753.5-0127. MNRAS 458:1636–1644. doi:10.1093/mnras/stw417. arXiv:1602.05816

Shaw AW, Charles PA, Bird AJ, Cornelisse R, Casares J, Lewis F, Muñoz-Darias T, Russell DM, Zurita C (2013) A 420-day X-ray/optical modulation and extended X-ray dips in the short-period transient Swift J1753.5-0127. MNRAS 433:740–745. doi:10.1093/mnras/stt763. arXiv:1303.6308

Shlosman I, Vitello P (1993) Winds from accretion disks - Ultraviolet line formation in cataclysmic variables. ApJ 409:372–386. doi:10.1086/172670

Silk J, Rees MJ (1998) Quasars and galaxy formation. A&A 331:L1–L4, arXiv:arXiv:astro-ph/9801013

Silva C, Uttley P, Costantini E (2015) Timing the warm absorber in NGC4051. In: The Extremes of Black Hole Accretion, p 63

Sim SA, Drew JE, Long KS (2005) Two-dimensional Monte Carlo simulations of HI line formation in massive young stellar object disc winds. MNRAS 363:615–627. doi:10.1111/j.1365-2966.2005.09472.x. arXiv:arXiv:astro-ph/0508103

Sim SA, Long KS, Miller L, Turner TJ (2008) Multidimensional modelling of X-ray spectra for AGN accretion disc outflows. MNRAS 388:611–624. doi:10.1111/j.1365-2966.2008.13466.x. arXiv:0805.2251

Sim SA, Miller L, Long KS, Turner TJ, Reeves JN (2010a) Multidimensional modelling of X-ray spectra for AGN accretion disc outflows - II. MNRAS 404:1369–1384. doi:10.1111/j.1365-2966.2010.16396.x. arXiv:1002.0544

Sim SA, Proga D, Miller L, Long KS, Turner TJ (2010b) Multidimensional modelling of X-ray spectra for AGN accretion disc outflows - III. MNRAS 408:1396–1408. doi:10.1111/j.1365-2966.2010.17215.x. arXiv:1006.3449

Simon LE, Hamann F (2010) The origins of a rich absorption line complex in a quasar at redshift 3.45. MNRAS 409:269–283. doi:10.1111/j.1365-2966.2010.17306.x. arXiv:1007.2017

Sluse D, Hutsemékers D, Anguita T, Braibant L, Riaud P (2015) Evidence for two spatially separated UV continuum emitting regions in the Cloverleaf broad absorption line quasar. ArXiv e-prints arXiv:1508.05394

Soleri P, Muñoz-Darias T, Motta S, Belloni T, Casella P, Méndez M, Altamirano D, Linares M, Wijnands R, Fender R, van der Klis M (2013) A complex state transition from the black hole candidate Swift J1753.5-0127. MNRAS 429:1244–1257. doi:10.1093/mnras/sts405. arXiv:1211.3537

Somerville RS, Primack JR, Faber SM (2001) The nature of high-redshift galaxies. MNRAS 320:504–528. doi:10.1046/j.1365-8711.2001.03975.x. arXiv:astro-ph/9806228

Springel V, Di Matteo T, Hernquist L (2005) Black Holes in Galaxy Mergers: The Formation of Red Elliptical Galaxies. ApJ Letters 620:L79–L82. doi:10.1086/428772. arXiv:astro-ph/0409436

Stalin CS, Srianand R, Petitjean P (2011) X-ray and optical properties of broad absorption line quasars in the Canada-France-Hawaii Telescope Legacy Survey. MNRAS 413:1013–1023. doi:10.1111/j.1365-2966.2010.18190.x. arXiv:1012.2425

Strateva I, Ivezić Ž, Knapp GR, Narayanan VK, Strauss MA, Gunn JE, Lupton RH, Schlegel D, Bahcall NA, Brinkmann J, Brunner RJ, Budavári T, Csabai I, Castander FJ, Doi M, Fukugita M, Győry Z, Hamabe M, Hennessy G, Ichikawa T, Kunszt PZ, Lamb DQ, McKay TA, Okamura S, Racusin J, Sekiguchi M, Schneider DP, Shimasaku K, York D (2001) Color Separation of Galaxy Types in the Sloan Digital Sky Survey Imaging Data. AJ 122:1861–1874. doi:10.1086/323301. arXiv:astro-ph/0107201

Surdej J, Hutsemekers D (1987) Geometry of the mass-outflows around broad absorption line QSOs and formation of the complex Ly-alpha + N V line profile. A&A 177:42–50

Šurlan B, Hamann WR, Kubát J, Oskinova LM, Feldmeier A (2012) Three-dimensional radiative transfer in clumped hot star winds. I. Influence of clumping on the resonance line formation. A&A 541:A37. doi:10.1051/0004-6361/201118590. arXiv:1202.4787

Tanaka Y, Ueda Y, Boller T (2003) ASCA observation of a dip of GRO J1655–40: evidence for partial covering and its implication. MNRAS 338:L1–L6. doi:10.1046/j.1365-8711.2003.06110.x

Tombesi F, Cappi M, Reeves JN, Palumbo GGC, Yaqoob T, Braito V, Dadina M (2010) Evidence for ultra-fast outflows in radio-quiet AGNs. I. Detection and statistical incidence of Fe K-shell absorption lines. A&A 521:A57. doi:10.1051/0004-6361/200913440. arXiv:1006.2858

Tombesi F, Meléndez M, Veilleux S, Reeves JN, González-Alfonso E, Reynolds CS (2015) Wind from the black-hole accretion disk driving a molecular outflow in an active galaxy. Nature 519:436–438. doi:10.1038/nature14261. arXiv:1501.07664

Trump JR, Hall PB, Reichard TA, Richards GT, Schneider DP, Vanden Berk DE, Knapp GR, Anderson SF, Fan X, Brinkman J, Kleinman SJ, Nitta A (2006) A Catalog of Broad Absorption Line Quasars from the Sloan Digital Sky Survey Third Data Release. ApJs 165:1–18. doi:10.1086/503834. arXiv:astro-ph/0603070

Ueda Y, Inoue H, Tanaka Y, Ebisawa K, Nagase F, Kotani T, Gehrels N (1998) Detection of Absorption-Line Features in the X-Ray Spectra of the Galactic Superluminal Source GRO J1655–40. ApJ 492:782–787. doi:10.1086/305063

Ustyugova GV, Koldoba AV, Romanova MM, Chechetkin VM, Lovelace RVE (1999) Magnetocentrifugally Driven Winds: Comparison of MHD Simulations with Theory. ApJ 516:221–235. doi:10.1086/307093. arXiv:astro-ph/9812284

van der Hooft F, Heemskerk MHM, Alberts F, van Paradijs J (1998) The quiescence optical light curve of Nova Scorpii 1994 (=GRO J1655–40). A&A 329:538–550 arXiv:astro-ph/9709151

Voit GM, Weymann RJ, Korista KT (1993) Low-ionization broad absorption lines in quasars. ApJ 413:95–109. doi:10.1086/172980

Walton DJ, Miller JM, Harrison FA, Fabian AC, Roberts TP, Middleton MJ, Reis RC (2013) X-Ray Outflows and Super-Eddington Accretion in the Ultraluminous X-Ray Source Holmberg IX X-1. ApJ Letters 773:L9. doi:10.1088/2041-8205/773/1/L9. arXiv:1306.2317

Warner B (2003) Cataclysmic Variable Stars. DOI. doi:10.1017/CB09780511586491

Weymann RJ, Morris SL, Foltz CB, Hewett PC (1991) Comparisons of the emission-line and continuum properties of broad absorption line and normal quasi-stellar objects. ApJ 373:23–53. doi:10.1086/170020

Woods DT, Klein RI, Castor JI, McKee CF, Bell JB (1996) X-Ray-heated Coronae and Winds from Accretion Disks: Time-dependent Two-dimensional Hydrodynamics with Adaptive Mesh Refinement. ApJ 461:767. doi:10.1086/177101

Yong SY, Webster RL, King AL (2016) Black Hole Mass Estimation: How Good is the Virial Estimate? PASA 33:e009. doi:10.1017/pasa.2016.8. arXiv:1602.04672

Zhou H, Wang T, Wang H, Wang J, Yuan W, Lu Y (2006) Polar Outflows in Six Broad Absorption Line Quasars. ApJ 639:716–723. doi:10.1086/499768. arXiv:astro-ph/0510243

Zubovas K, King A (2013) BAL QSOs and Extreme UFOs: The Eddington Connection. ApJ 769:51. doi:10.1088/0004-637X/769/1/51. arXiv:1304.1691

http://www.springer.com/978-3-319-59182-7

Disc Winds Matter
Modelling Accretion and Outflows on All Scales
Matthews, J.
2017, XXXVIII, 210 p. 93 illus., 63 illus. in color.,
Hardcover
ISBN: 978-3-319-59182-7